

Observing with the Wide Field Spectrograph (WiFeS) – Version 1.3

Michael Dopita

© Springer-Verlag ●●●

Abstract This document provides an introduction to the Wide Field Spectrograph (WiFeS) instrument, its observing modes, capabilities and to the required calibration observations. It has been prepared by the project scientist, Emeritus Professor Michael Dopita. Any questions, comments or grouses should be addressed to: Michael.Dopita@anu.edu.au.

Sections 2–9 describing the instrument are adapted from the paper:

Dopita, M., Hart, J, McGregor, P., Oates, P & Jones, D. 2007, *"The Wide Field Spectrograph (WiFeS)"*, Ap&SS, 310, 255.

That paper must be referenced in any paper which has used observations obtained with the WiFeS instrument.

Important Notice: During their observational run observers must not touch or alter any part of the instrument or its electrical connections. Failure to observe this notice may result in irreparable damage to the instrument. Observers must seek technical assistance in the case of any and all instrument problems.

Michael Dopita

Research School of Astronomy & Astrophysics, Australian National University, Cotter Rd., Weston ACT, Australia 2611

Contents		14.3 Wavelength Calibration	29
		14.4 Flux Calibration	29
1 Instrument Description	3	15 WiFeS data reduction pipeline	31
2 Introduction	3	15.1 Overview	31
3 Science Drivers & Design Philosophy	3	16 Installing the package	32
4 Instrumental Overview	5	17 Setting up for data reduction	32
5 Optical Considerations	7	18 WiFeS data format	33
5.1 Concentric Image Slicer Geometry . . .	7	19 WiFeS Data Reduction	34
5.2 Gratings & Resolution	7	20 WiFeS Pipeline Scripts	36
5.3 Camera Design	7	20.1 WFTABLE: Setting up for data re-	
6 Mechanical Design	8	duction	36
7 Throughput	12	20.2 WFCAL : Calibrating the Data . .	37
7.1 Mirrors	12	20.3 WFREDUCE: Reducing the Data .	38
7.2 Dichroics	14	20.4 Description of Reduction Procedures	41
7.3 Gratings	14		
7.4 Cameras	15		
7.5 Detectors	15		
8 System Throughput	15		
8.1 System Sensitivity	16		
9 Image Quality	17		
10 Summary	17		
11 WiFeS Observing	20		
11.1 Getting Started under CICADA . .	20		
11.2 In case of CICADA Crash	20		
11.3 Additional Advice	20		
11.4 The WiFeS Observation Sequence			
Window	22		
12 Acquisition & Guiding	22		
12.1 Pre-observing set up	24		
12.2 Basic Acquisition	24		
12.3 Bright Point Source Acquisition . .	25		
12.4 Faint Point Source Acquisition . . .	26		
12.5 Extended Source Acquisition	26		
13 Data Accumulation Modes	27		
13.1 Classical Mode with Equal Exposures	27		
13.2 Classical Mode with Unequal Ex-			
posures	27		
13.3 Nod-and-Shuffle Mode with Equal			
Exposures	27		
13.4 Sub-Aperture Nod-and-Shuffle . .	28		
14 Calibration of Data	29		
14.1 Flat-Field Calibration	29		
14.2 Aperture Calibration	29		

1 Instrument Description

2 Introduction

An integral field spectrograph is an instrument designed to obtain a spectrum for each of the spatial elements it accepts. In this sense, a classical long-slit spectrograph could also be regarded as an integral-field spectrograph. However, its field shape is rather inconvenient for many practical purposes, being limited to one spatial element in the dispersion direction. The basic problem in designing a grating approach to an integral field spectrograph is therefore to re-format the entrance aperture to allow the acceptance of a convenient 2-D array of spatial elements.

Broadly speaking, three approaches have been applied to the problem of integral field spectroscopy, which can also be referred to as hyper-spectral imaging. These are, micro-lens array pupil imaging (as in the SAURON spectrograph (Bacon et al. 2001), micro-lens arrays coupled to fibre spectrograph feeds (Arribas & Mediavilla 2000; Roth et al. 2000), and optical image-slicing (Content 2000).

Each of these have different strengths and weaknesses. The micro-lens array pupil imaging approach allows an instrument of very high throughput, but has a problem of separating the spectra of the individual spatial elements from each other on the detector. This leads to limited spectral coverage, an inefficient use of the detector real estate, and the data reduction is difficult.

The fiber-coupled approach as exploited, for example, in the AAOMEGA spectrograph (Saunders et al. 2004) allows for a free formatting of the spatial elements on the sky, either as a multi-object spectrograph, or as a filled aperture integral field device. The data formatting with this type of device is very convenient, looking very much like a standard long-slit spectrograph, and allowing for easy data reduction. However, the f-ratio of the beam entering the fibers is often large, and any curvature in the fibers will re-distribute the light in an unpredictable way within the effective f-ratio of the fibers themselves. Thus, in order to capture the emergent beam, the f-ratios of the collimator and camera must also be small, which leads to difficult optics design. Variable (and wavelength dependent) fiber throughput and output beam characteristics can lead to a difficult and sometimes unpredictable spectrophotometric calibration and performance.

The image-slicing approach has the advantage of preserving the input f-ratio, and provides a convenient data format. However, depending on the slicer optics, it may produce a field-dependent image quality. However, this

problem can be avoided using the “concentric” image-slicer concept as first applied to the NIFS instrument located Gemini North (McGregor et al. 1999, 2003), and now producing exciting science results (McGregor et al. 2007).

The success of the Systemic Infrastructure Initiative proposal for the upgrade of the ANU and UNSW telescopes at Siding Spring Observatory (SSO) enabled us to undertake the construction of an entirely new spectroscopic instrument to be mounted at one of the Nasmyth Focii of the 2.3m telescope. It is designed to take maximal advantage of the properties of that telescope while providing a much greater efficiency than the previously available Double Beam Spectrograph (DBS) Rodgers, Conroy & Bloxham (1988). This paper describes the science drivers, design philosophy, optics and mechanical implementation and the expected on-telescope performance characteristics of this **W**I**D**e **F**i**E**ld **S**pectrograph (WiFeS).

3 Science Drivers & Design Philosophy

The 2.3m telescope at Siding Spring Observatory is a relatively modest-sized telescope, with a rather restrictive (~ 6 arc min.) unvignetted field of field. The science mission of any new 2.3m instrument should therefore be motivated by the requirement to do exciting and internationally competitive science. This immediately limits the possible instruments to one of two kinds:

- Niche instruments designed to do a timely class of science very efficiently, *or*
- An efficient facility-class instrument designed to provide a versatile capability over a whole range of scientific objectives.

The research and research training mission of the RSAA and of the other user institutions demands the choice of second type of instrument in order to benefit the greatest user community. In particular, the Australian user community is looking for a versatile, stable and efficient instrument which provides not only excellent performance on extended objects, but which can also be used for spectroscopy of single stellar sources with an efficiency appreciably greater than the previously available Double Beam Spectrograph (DBS) Rodgers, Conroy & Bloxham (1988).

The science mission that is enabled by such an instrument is very broad. Galactic studies include the internal dynamical studies to investigate mergers, and to study the rotation curves of dwarf galaxies to resolve the core-cusp controversy. The H II regions in galaxies will be studied to measure abundances and abundance

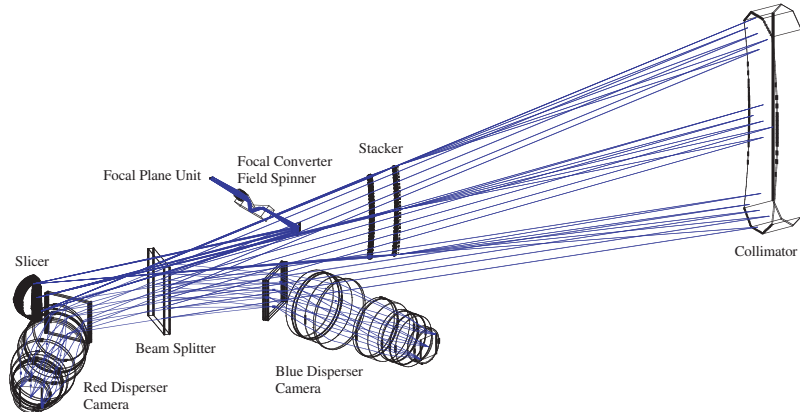


Fig. 1.— The general optical configuration of the WiFeS spectrograph. Light passes from the field definition dekker through the de-rotator and f-ratio change optics, and is folded through 90 degrees for packaging reasons. An image of the entrance slot is projected onto the image slicer which fans each slice concentrically to form a set of pupils stacked vertically above one another. The ‘stacker’ refocusses the light to form a set of slit images equally spaced on a spherical surface. A slit mask placed here eliminates scattered light. The light is then collimated by a spherical collimator, and on its return path passes through a dichroic before forming a ‘blue’ and a ‘red’ pupil on VPH gratings. All gratings are fixed at Littrow and run at the same angle of deviation.

gradients from strong lines, weak lines and recombination lines to resolve the origin of the discrepancies between these three methods. The stellar component of galaxies will be studied to derive spatially resolved spectral energy distributions (SEDs), attenuation by dust, and local star formation rates in starburst galaxies and circum-nuclear star-forming regions. The gas kinematics and excitation around active nuclei will be studied to provide physical conditions in the ISM of these regions, to quantify the photon and mechanical energy output from the central object. In a few cases it may be possible to estimate the black hole mass. At high redshifts, we would like to study the dynamics of the extensive Ly- α halos seen round distant radio galaxies, and to study the interstellar or inter-galactic absorption features seen in the GRB sources.

In stellar studies we would like to investigate single stars, especially those hosting planetary systems, and perform studies of the evolution of the early galaxy by observing very metal-poor star candidates identified in surveys, investigating old stellar streams in the halo to investigate the merging history of the Galaxy, to obtain spectroscopy of many stars in a single exposure in Galactic globular clusters, and also to study clusters in the Magellanic Clouds.

Finally ISM studies include the investigation of the internal structure, excitation and dynamics of planetary nebulae and old nova shells, making abundance analyses of extra-galactic H II regions as described above, mapping the dynamics and heavy element content of supernova remnants, and studying the outflows seen in Herbig-Haro objects.

These science drivers define the following set of basic science requirements for the spectrograph:

- An integral field $\sim 30 \times 30$ arc sec. or greater.
- Excellent stability of the spectrograph in both the spatial and spectral planes.
- High spectrophotometric veracity ($< 1\%$) and excellent sky-subtraction capability.
- The provision of a pipeline data reduction capability and calibration libraries.
- An ability to cover full spectral range with a single exposure at a resolution $R > 2000$.
- The provision of an intermediate resolution mode offering $R \sim 7000$.

The WiFeS spectrograph was designed around the science mission to provide all of these capabilities. Specifically, we have maximized the Felgett Multiplex Advantage; the number of independent spectral and spatial resolution elements. We maximize the detector real estate, compatible with optical constraints and match the spatial resolution to the seeing. The detector scale is 0.5 arc sec per pixel, and the slices are each 1.0 arc sec wide. The Jaquinot Advantage, sometimes known as the luminosity resolution product (Jaquinot 1960) is also maximized. The luminosity of an instrument is measured by the product of the étendu, the solid angle accepted without degradation of the resolution, and the throughput of the instrument. The étendu is determined by the nature of the dispersive element. Throughput is maximized by the choice of technology of the coatings and materials of the optical train and in the detector.

Finally, we aim to maximize the science data gathering and evaluation efficiency by providing an instrument with high spectrophotometric stability, simple calibration procedures and operating modes, calibration libraries, efficient feedback of data quality to observer, and batch data reduction to produce standardized data products.

4 Instrumental Overview

The WiFeS instrument, scheduled for completion at the end of 2007 draws upon the design heritage of both the DBS Rodgers, Conroy & Bloxham (1988) and the concentric image-slicer concept of the NIFS instrument for Gemini North McGregor et al. (1999, 2003). The instrument is designed to deliver as many simultaneous spectra as possible, each covering as wide a spectral range as possible. This predicates the use of a dichroic beamsplitter in front of two gratings and their associated cameras.

The science requirements mandate the use of large-format detectors to provide the required spatial and spectral coverage, but ultimately the maximum field and spectral coverage equally limited by both optical design considerations and mass, and physical packaging constraints. The detector format for both the “blue” and the “red” cameras is 4096×4096 with a pixel size of $15\mu\text{m}$ square. The need to provide a nod-and-shuffle capability for sky subtraction (which requires half the detector real estate for the object exposures and the other half for the sky reference exposures), together with the need to properly sample the image (2 pixels) in both the spatial and spectral domains, limits the independent spectral pixels to 8192 and spatial pixels to 1900 per exposure, respectively.

The optical design aims to critically sample the point spread function delivered by the telescope and the average seeing at Siding Spring, implying a 0.5 arc sec spatial pixel. It also aims to critically sample each resolution element in the spectral domain. Each 1.0 arc sec wide slice is therefore designed to project to 2 pixels on the detector, and the dispersion is chosen to give a resolution which is well-matched to the slit width.

Since we wish to provide a relatively simple data reduction pipeline and an instrument with excellent spectrophotometric precision ($< 1\%$), the use of fibre-optics were avoided. Instead, a concentric image-slicer design utilising “long-slit” slitlets was adopted. This concept is shown in Figure 1.

The requirement for excellent stability of the spectrograph precludes rotation the instrument with the field rotation at the Nasmyth focus. Therefore an Abbé-König derotator prism is placed just behind the entrance slot mask. The doublet f-ratio conversion lens optically coupled to this avoids an extra air-glass surface.

The requirements for high throughput and good broad-band response predicates the use of transmissive optics where possible, application of optimised optical coating materials, the use of high-efficiency volume phase holographic (VPH) gratings, and a double-beam operational capability with separate cameras to maximize response in both the “blue” and the “red” arms and have the capability to collect data from both arms simultaneously.

The concentric image-slicer is a macroscopic version of the concept used in the NIFS spectrograph, with the physical width of each slice being 1.75 mm. The image rotator is manufactured as a set of identical 1.75 mm thick half cylindrical plates sandwiched between thicker slabs of glass of the same form. These are held together in a mandril which applies the lateral pressure and locates all the hemispheres in a vee groove. The multi-element front surface is ground and polished to the correct spherical figure. The wax is individual slices are fanned out using a pair of adjustment screws at the ends of each one. The vee groove ensures that each slice is rotated about its front face. The fanned slicer is then compressed in the mandril, and coated to provide high reflectance. The final image slicer in its fanned position is illustrated in Figure 2.

The image-slicer forms a set of 25 pupils, one for each slice, stacked vertically above one another on the surface of a sphere centred on the slicer. An achromatic doublet lens and a singlet field lens then forms a row of images of each slitlet on a sphere again centered on the slicer. At this point a slit mask is placed to baffle any stray light in the system. We call this unit the ‘stacker’.

The row of slit images is formed half-way between the slicer and the collimator. In this configuration, the ray bundle associated with each slitlet strikes the collimator at normal incidence and the returning collimated beams from all slitlets form a common pupil at the plane of the grating which is co-planar with the image slicer. By minimizing off-axis angles, this ‘concentric’ approach ensures excellent and uniform image quality across the field.

The slicer and stacker presents to the WiFeS spectrograph what is in effect a very long-slit format with separated segments corresponding to each slice. Indeed, the effective slit is so long that field angle effects on the grating are appreciable. The fan angle on the image slicer is chosen so that the slitlet image at the stacker is separated by just over its own length from its neighbours. Together these provide an image format on the detector shown in Figure 3.

This format may look wasteful from the viewpoint of efficient use of the detector real estate, but it does offer a notable advantage for the detection of very faint objects, since it allows for what we have termed “interleaved nod-and-shuffle” on the CCD. The technique of nod-and-shuffle is well-developed Cuillandre (1994); Tinney (2000); Glazebrook (2001), and provides for excellent sky-subtraction because, for any spatial or spectral position, both object and sky are observed virtually at the same time, for the same time, and on the same pixel. This allows for \sqrt{N} statistics in the removal of unwanted sky signal from the object signal.

The implementation of nod-and-shuffle in WiFeS is to expose for a short period of time, typically 30s. The shutters are closed, and the charge on the CCDs transferred in the x -direction by the width of each slitlet (Δx pixels) to move the object signals into the inter-slit space. The telescope is nodded to the reference sky position and a sub-exposure of the same length is taken. The shutter is again closed, charge shuffled back to its original coordinate, and the telescope returned to the target position. The whole process is then repeated as many times as necessary. Sky subtraction is achieved by subtracting each part of object signal from the signal located Δx pixels from the object signal. An on-frame bias signal is provided along the chip edge where the charge shuffling causes charge to be repeatedly lost ‘overboard’.

Since there remains a risk that the de-rotator axis and the telescope field rotation axis are not precisely aligned, both offset guiding and through entrance slot acquisition cameras are provided (but not shown in Figure 1). The second camera is fed by a flip mirror immediately in front of, and mechanically coupled to, the image slicer. This enables the observer to re-centre the

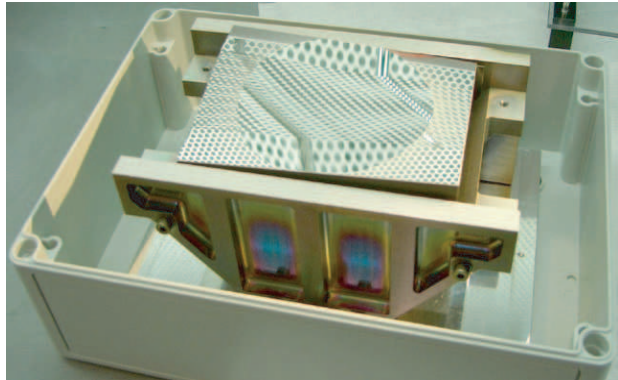


Fig. 2.— The WiFeS image slicer in its final fanned configuration mounted in its mandril which also serves as a mounting block for the slicer in the instrument.

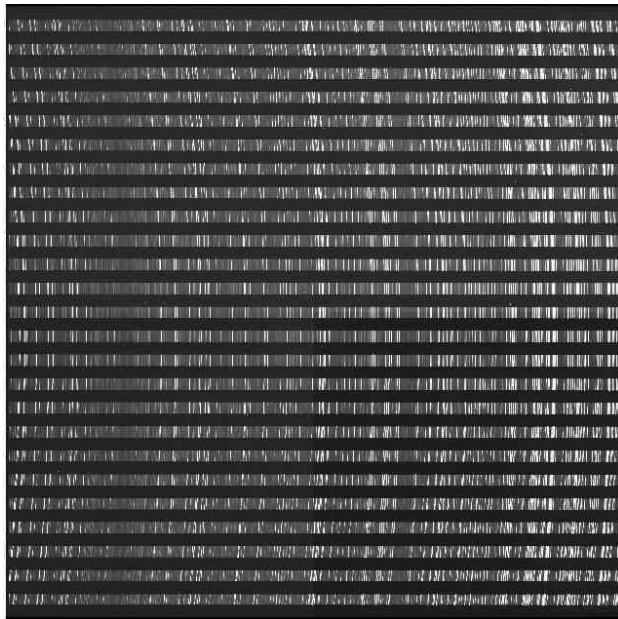


Fig. 3.— The image format on the detector for the B_{7000} grating. The long wavelength part of the spectrum is on the left. Other gratings give very similar formats, but the spectral dispersion direction is reversed in the red arm. Note the spaces between adjacent spectra allow ‘nod-and-shuffle’ sky subtraction to be achieved. The sky spectra are accumulated in these spaces, and sky subtraction is achieved by shifting the image with respect to itself by 80 pixels, and then subtracting it from the unshifted image.

stellar target or offset guide star precisely on the image slicer between science integrations to avoid any blur resulting from uncorrected field rotation.

5 Optical Considerations

5.1 Concentric Image Slicer Geometry

The basic geometrical conditions of the IFU and spectrograph are specified as follows. The diameter of the collimated beam in the spectrograph is dictated by the resolving power requirement. The high-resolution gratings operate at a grating angle of $\theta = 22^\circ$, and are required to provide a spectral resolving power of $R = 7000$. The VPH gratings operate in Littrow condition. For a telescope diameter of D_{tel} and an angular slit width of $\delta\phi_x$, the required collimator beam diameter, d_{coll} , is given by:

$$d_{\text{coll}} = \frac{D_{\text{tel}}\delta\phi_x R}{2 \tan \theta}. \quad (1)$$

With $D_{\text{tel}} = 2300\text{mm}$ and $\delta\phi_x = 1.0\text{arc sec.}$, we have $d_{\text{coll}} = 97\text{mm}$.

The angular field size is designated as $\Delta\phi_x$ in the spectral direction and $\Delta\phi_y$ in the spatial direction. The number of slices determines the aspect ratio of the field. We aim for an aspect ratio ~ 1.5 to provide a good format for astronomical observation. With our choice of $N = 25$ slices, a sampling of 2 pixels per slit, and a small clearance margin at the edge of the detector, the number of pixels used in the spatial direction is $n_{\text{spatial}} = 4080$. For an anamorphic magnification of $M = 1$ (the Littrow condition), the maximum angular field size in the spatial direction is:

$$\Delta\phi_y = \frac{n_{\text{spatial}} M 2(2N + 1)}{\delta} \phi_x. \quad (2)$$

This limits the maximum slit length to 40 arc sec. on the sky. The angular field size in the spectral direction is then $\Delta\phi_x = N\delta\phi_x = 25\text{arc sec.}$, giving an aspect ratio of 1.6.

At the detector, the width of the spectra is 80 pixels. In order to provide the ability for nod-and-shuffle (see below) this spatial field is masked down to 38 arc sec. to provide gaps between spectra of 4 pixels, thus avoiding interference or overlap between the object spectra and the sky background spectra.

5.2 Gratings & Resolution

The design avoids the need to articulate the cameras. To ensure that the spectrograph resolution remains approximately constant for each grating, gratings operate

in first order, at Littrow and at a constant angle of deviation and deliver the same fractional free spectral range, $\Delta\lambda/\lambda$ to the detector in the high resolution mode $R = 7000$. This corresponds to a (two pixel) velocity resolution of 33 km.s^{-1} . In practice, the resolution is about 2.3 pixels, when the resolution of the grating and of the optics is folded in with the 1.0 arcsec. slit width. The resolutions achieved by the spectrograph are therefore $R = 6700$ corresponding to a velocity resolution of 45 km.s^{-1} in the high resolution mode. The dispersive elements are volume phase holographic (VPH) transmission gratings, individually manufactured to the requisite number of lines per mm. VPH gratings offer the notable advantage that their peak efficiencies can be greater than 90% when the substrate surfaces have been anti-reflection coated. In addition, each grating may be tilted somewhat in its mounting to optimise efficiency by tuning to the ‘superblaze’ peak.

In the WiFeS instrument, three gratings are mounted on a slide drive in each arm of the spectrograph, two high dispersion gratings with $R = 7000$ and one low dispersion grating. To provide for this lower resolution option ($R = 3000$ or a velocity resolution of 100 km.s^{-1}) we have coupled prisms to the two low-dispersion VPH gratings to match the deviation of the beam to the high-resolution case. The dispersions of the prism and the VPH grating work in opposite senses, so the VPH dispersion needed to be somewhat increased to compensate.

For any particular grating, the wavelength coverage and the format on the detector is fixed. This ensures that the data reduction pipeline can be standardised – essential if the instrument is to provide an efficient stream of reduced science data to the users. The “blue” arm is required to operate over the wavelength range 329 - 558 nm ($R = 7000$) and 329 - 590 nm ($R = 3000$), and the “red” camera in the 529 - 912 nm ($R = 7000$) and 530 - 980 nm ($R = 3000$). Two dichroics are used with the four high resolution gratings to avoid the cut-over wavelength region, and so provide high dichroic efficiency at all wavelengths. A third dichroic is used with the two resolution gratings. In this case, the lower efficiency in the region of the dichroic cut is compensated by a generous overlap in wavelength coverage between the blue and the red arms. The modes of operation offered by the WiFeS instrument are given in Table 1.

5.3 Camera Design

The spectrograph presents collimated light with a beam diameter of 97 mm, to two gratings simultaneously, *via* a beamsplitter. The dispersed spectra are imaged by two cameras. The “blue” camera is required optimized

Table 1 The WiFeS grating and dichroic set

Grating	U_{7000}	B_{7000}	R_{7000}	I_{7000}	B_{3000}	R_{3000}
Lines/mm	1948	1530	1210	937	708	398
λ_{\min} (Å)	3290	4184	5294	6832	3200	5300
λ_0 (Å)	3850	4900	6200	8000	4680	7420
λ_{\max} (Å)	4380	5580	7060	9120	5900	9800
Dichroic#	RT480	RT615	RT480	RT615	RT560	RT560
λ_{cut} (Å)	4850	6200	4850	6200	5600	5600

for operation over the wavelength range 329 - 557nm, and the “red” camera in the 557 - 900nm range. Each camera has a focal length of 261mm and each images onto a 4096×4096 CCD detector with $15\mu\text{m}$ square pixels. An important design cost driver requirement for the camera was that all surfaces should be spherical.

The Schott 2000 and OHARA 2002 catalogues were searched for glasses with good transmission properties down to 329 nm. These were tested against each other using their differential relative partial dispersions (dRPDs). It is essential to closely match dRPDs so that secondary colour and sphero-chromatism can be minimized. Also, in some cases, it is possible to use low-powered elements of more greatly differing dRPD to fine-tune the chromatic residuals. Two additional glasses, Calcium Fluoride and fused Silica, were also included in the glass suite because the former shows exceptionally low dispersion and the latter provides a very high transmission in the UV.

The final selection of glasses for the blue camera is: CaF₂; SCHOTT PSK3; OHARA S-FPL51Y, BSM51Y & S-LAL7; and fused Silica. This set delivers excellent transmission down to 329 nm with very good image quality over the entire band. Interestingly, there are far fewer well-matched glasses from which to choose for the red camera. This tends to be contrary to traditional expectations. A detailed examination of the dRPDs showed that, surprisingly, the OHARA glasses S-LAL7 and S-YGH51 were the best matches for OHARA S-FPL51Y (the core “crown”). CaF₂ becomes a progressively worse match for all these materials as one moves to longer wavelengths than 560 nm. The selections for the red glass set are OHARA S-FPL51Y, S-LAL7, S-YGH51 and fused Silica. Fused Silica is used to “fine tune” the chromatic residuals in both cameras.

The cameras both use a four-component Petzval system with a thick field flattener doubling as a Dewar window. The first component is a triplet, the second and third are singlets, the fourth is a quadruplet and the field flattener singlet serving as the window to the

cryostat. Neither camera is corrected for lateral colour, but this is not necessary in a spectrograph. However, the cameras are designed to correct the field distortion produced within the spectrograph. This ensures that each column on the detector corresponds to a unique spatial element – a great advantage in data reduction. The configuration of the camera is shown in Figure 4.

6 Mechanical Design

The basic mechanical design of WiFeS is that of a fixed rigid box structure kinematically mounted on a rigid box girder platform attached to the Nasmyth B focus of the 2.3m telescope. The rotation of the field is removed by a de-rotator module mounted on the field rotator between the telescope fork and the body of the spectrograph. The calibration lamps are carried in this module. The primary function of the de-rotator is to eliminate the image rotation that occurs as the telescope tracks a star field (field spinner). It also has the secondary functions of reflecting excess field image back to the guider (focal plane unit), and reeling the electrical cables that serve itself and the guider (cable wrap).

The requirement that the spectrograph remains with fixed gravity loading is driven by the need to maintain a high spatial stability of the individual spectra on the detectors. The fixed orientation eliminates the flexure that would occur in a spectrograph free to rotate. In the case of the existing DBS, which is a spectrograph of similar size to WiFeS, this flexure leads to as much as 8 pixels of movement – a quite unacceptable figure.

The problem with our adopted design is that the spectrograph is quite a long way from the face of the fork of the telescope. The major consideration in the design of WiFeS has been the conflicting needs for both high stiffness and low moment load. The stiffness requirement arises from the need to keep natural vibration frequencies high relative those of the telescope and

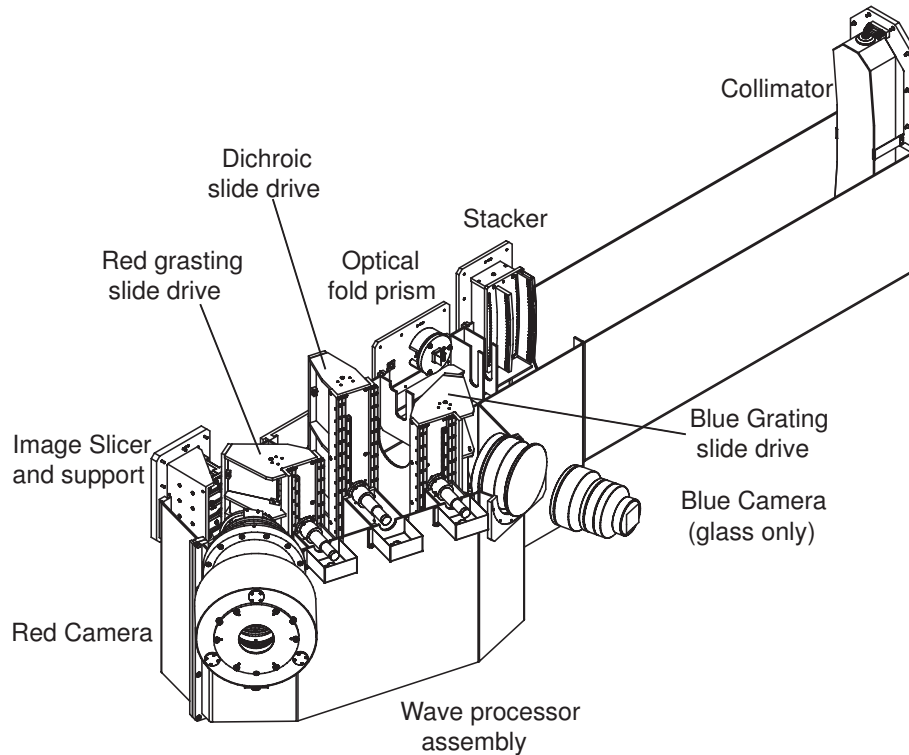


Fig. 5.— The overall mechanical configuration of the WiFeS spectrograph.

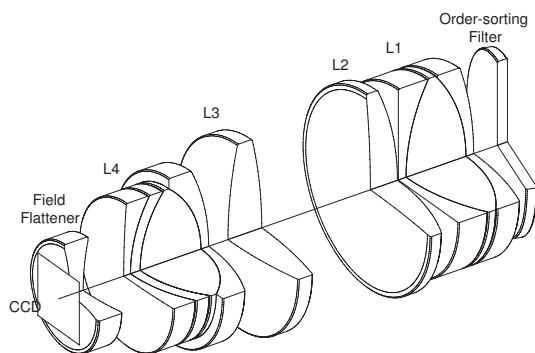


Fig. 4.— The optical configuration of the $f/2.69$ red camera for the WiFeS spectrograph. The blue camera configuration is very similar

so preserve telescope dynamic performance. The moment limit arises from the need to restrict eccentric loading on the azimuth bearing of the telescope and so preserve its operational life. The configuration chosen for WiFeS makes it difficult to achieve these requirements. In particular:

- The spectrograph has been made stationary in orientation as a means of achieving optical stability. This has required the addition of an optical de-rotator that adds weight and complexity.
- The spectrograph is displaced a long way from the fork in order to accommodate the instrument rotator, guider and de-rotator. The rotating nature of these components precludes use of an axial support system for the spectrograph, requiring the addition of a long cantilever mount. This cantilever must be slender to fit within the available space. Load moment and stiffness are then more problematic.
- The collimator takes the form of an uncorrected spherical mirror in order to maximise throughput. This limits its focal ratio and makes the spectrograph unusually long and heavy. The concentric IFU also makes the collimator mirror unusually large.

- A comprehensive suite of remotely deployable beam splitter and disperser elements makes the spectrograph unusually tall and heavy.

Careful design has resulted in a load moment of 1503 kg m about the telescope centre, which does not significantly exceed the limit of 1500 kg m. This corresponds to an azimuth bearing lifetime of 77 years when the telescope is operating with its Caspir on Cassegrain and Imager on Nasmyth B, and 63 years for the worst-case loading of full Cassegrain and empty Nasmyth B.

Likewise, acceptable stiffness has been achieved. The lowest translational natural frequency (vertical cantilever flexure) is 59 Hz. The lowest rotational natural frequency (cantilever torsion) is 33 Hz. As required, these values are larger than the lowest natural frequency of the telescope, which is 11 Hz. The associated maximum deflection due to vertical cantilever flexure is 0.072 mm negligible relative to the linear image resolution in this domain of 1.75 mm (this being the slit width).

Finally, the differential thermal expansion in the vertical plane over the operating temperature range of 0 – 20°C will move the spectrograph vertically with respect to the optical axis. For a steel telescope fork and aluminium alloy spectrograph housing, the maximum shift is 0.12 mm. This also has a negligible effect on image stability.

The overall mechanical layout of the spectrograph body is shown in Figure 5. Note the kinematic truss mounting of the collimator, and the way that the vee groove mandril support for the image slicer is incorporated into the mounting.

Note also the stacker, consisting of doublet pupil lenses, singlet field lenses, and slit image mask. This arrangement serves to capture stray light from the slicer, contributing to the excellent contrast expected in the final images. The pupil and field lenses have diameters of 9 and 10 mm respectively. All are retained in close-fitting bore holes by custom made snap rings and wave springs. With the nod-and-shuffle observing technique, the slitlet images have an angular size about the fanning axis that is slightly smaller than half the angular channel fanning pitch. This is illustrated by the separation of the perforations in the field mask. It also provides enough space between the channels to accommodate lenses that must be larger than their beam apertures.

The spherical collimator mirror has its radius of curvature centered on the fanning axis of the image slicer. It is slightly inclined so as to separate the pupil plane from the fanning plane. It is suspended on three triangular trusses. These are flexible in all deflection modes except translation in the truss plane. Together, they

act as a kinematic hexapod. In addition, two brackets are supplied at mid section as safety devices that prevent the mirror from falling forward in the event of support failure. The hexapod trusses have a vertical stiffness is 40400 N/mm. For the mirror mass of 19 kg, this gives a natural vibration frequency of 1460 Hz – very much higher than the lowest natural frequency of the telescope (11 Hz). Vibration will therefore not be excited.

The details of the wave processor assembly are shown in Figure 6. The grating and dichroics are mounted at fixed angles on slide drives which drive gratings in the direction perpendicular to the dispersion so that gratings can be rapidly exchanged with the assurance that the previous wavelength and spectrophotometric calibrations remain unchanged. Note how the low dispersion grisms are mounted in the centre of each grating drive assembly. The box plus box girder construction makes this assembly exceedingly rigid.

The red camera is shown in Figure 7. Although the red and blue cameras have different optical prescriptions, they use the same mechanical design approach. The field flattener with its mounting plate is physically part of the cryostat module, where it acts as the vacuum window. The mechanical structure is aluminium alloy with thin-walled cylindrical forms to achieve high stiffness and low weight. All components of multiplet lenses are oil-coupled. Circumferential o-ring seals are used to contain the oil, and volumetric compensation is provided to account for oil displacement caused by differential thermal strain, which leads to small differential changes in radii of curvature. Although these have no effect on image quality, they may lead to separation of the components, if not accommodated for.

Camera focus is accommodated with a focus stage carried on three lead screws equi-spaced on a pitch circle of 135 mm radius. Each lead screw has a pitch of 1 mm and can rotate through almost one revolution between limit switches. The travel range is therefore almost 1 mm. This is sufficient to correct temperature effects and minor errors in detector position. The three screws are independently motorized through a high reduction gearhead, and encoded. They therefore also provide tip-tilt adjustment. The drive time taken to traverse the whole range is about 30 seconds.

The detectors are mounted in the red and blue cryostats which are mechanically identical except for the vacuum window / field flattener lens. Cryocooling is provided by commercial CryoTiger closed-cycle refrigeration systems. These include remotely mounted air-cooled compressors with refrigerant lines to PT14 high performance cold heads mounted in the cryostats. These have a cooling power of 11.5 W at 94°K.

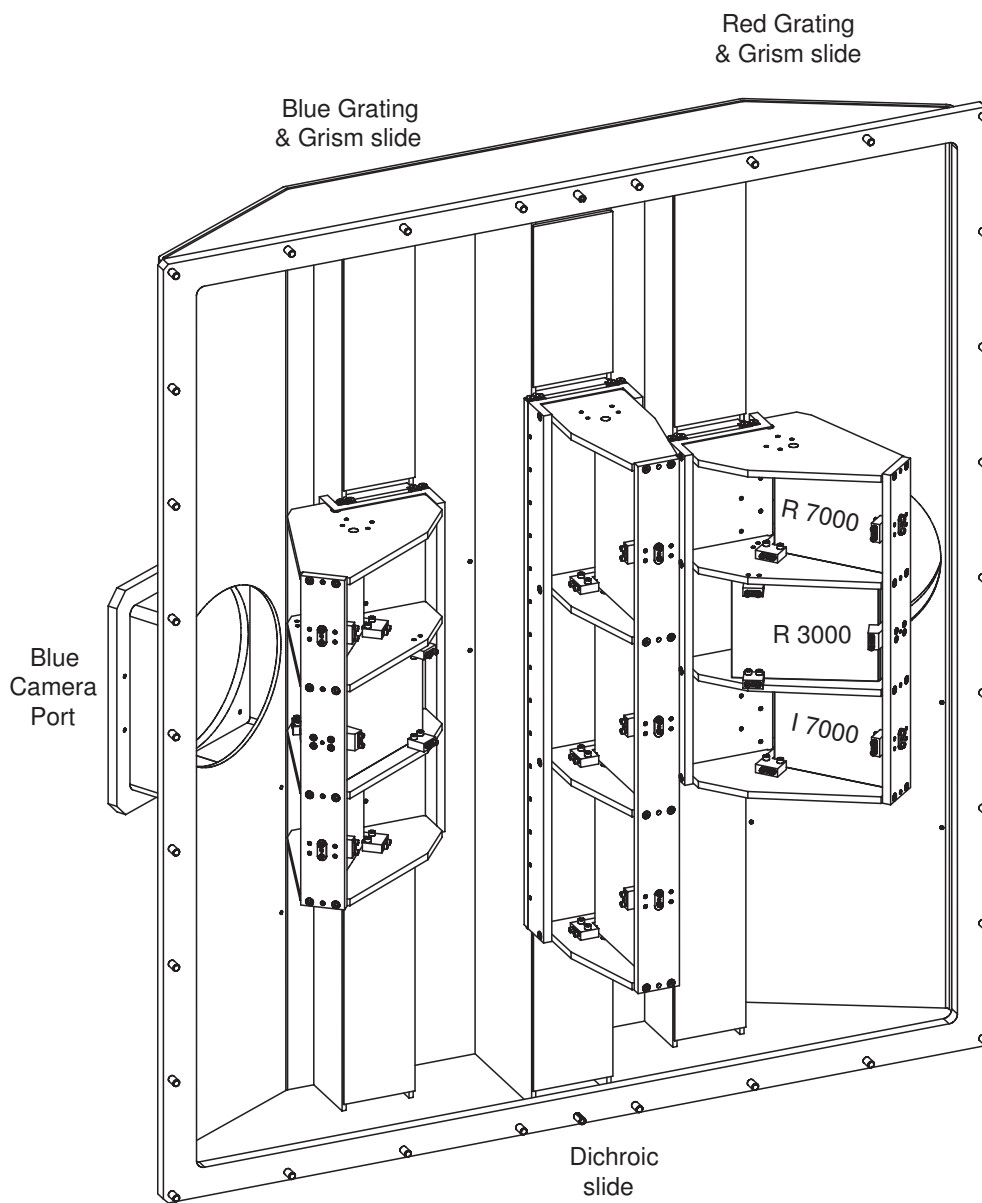


Fig. 6.— The mechanical configuration of the wave processor assembly. The gratings and dichroics are permanently mounted on the slide-drives in the wave processor assembly, ensuring stability of the wavelength calibration and reproducibility of the flux calibration.

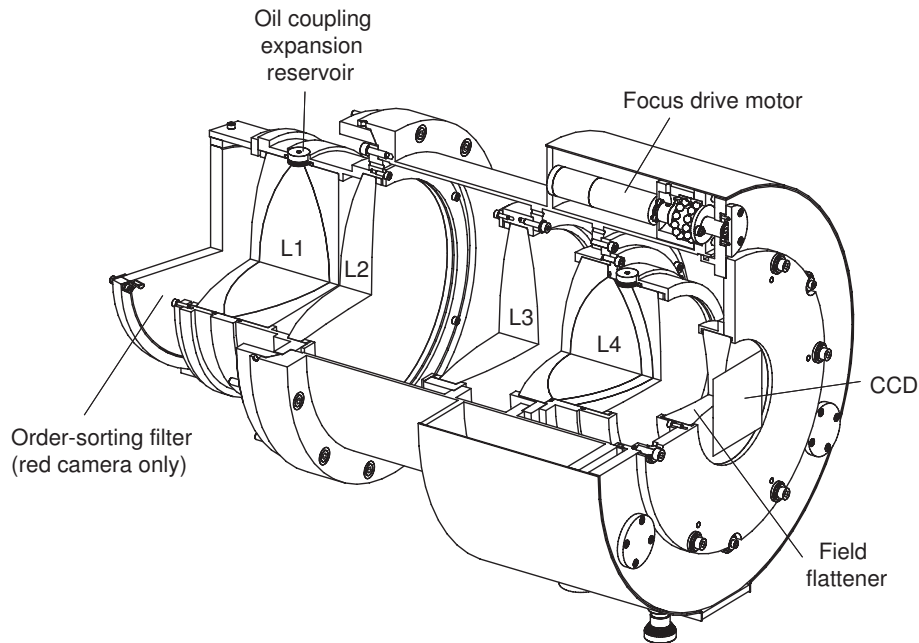


Fig. 7.— The mechanical configuration of the camera. Here the thermal stability is paramount, and the differential expansion of the glasses in the compound lenses must be accommodated by the oil coupling, as described in the text. The thermal compensation of the camera is accomplished by the combination of a passive “thermal bellows” (not shown) which moves L3, and a change in the camera focus. This ensures that the image scale is invariant with temperature.

7 Throughput

The need to maximize the Jaquinot advantage requires optimal throughput performance. The WiFeS spectrograph delivers an extraordinary throughput, with peak transmission (including atmosphere, telescope, spectrograph and detector) peaking above 40%, with $> 30\%$ in the wavelength range 450 - 850 nm, and $> 20\%$ in the wavelength range 370 - 900 nm. It exceeds the throughput of the DBS spectrograph, the spectrograph which it replaces, by typically a factor of three. This has been achieved by an aggressive effort to choose the optimum technological solution for each element throughout the optical train. The key elements of this effort will now be briefly described.

7.1 Mirrors

For WiFeS, we have employed the broad-band Lawrence Livermore protected silver coating developed by Jesse Wolfe and David Sanders at LLNL (Wolfe & Sanders 2004). These were developed for the National Ignition Facility and have most notably been used on the Keck telescope Thomas, Wolfe & Farmer (1998). This coating is very durable, passing such tests such as boiling

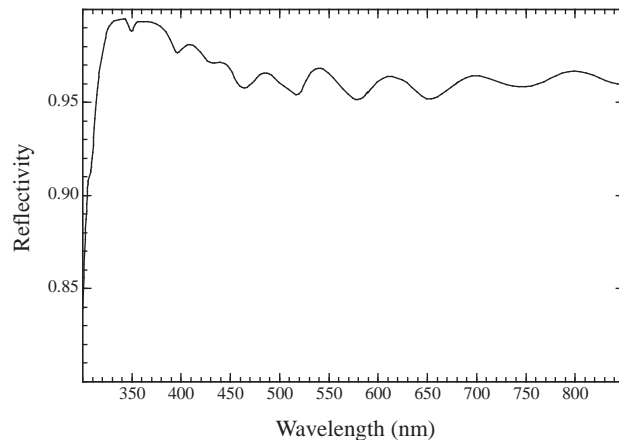


Fig. 8.— The measured reflectivity of the LLNL coatings employed for the WiFeS mirrors. At all wavelengths the reflectivity is greater than 95%.

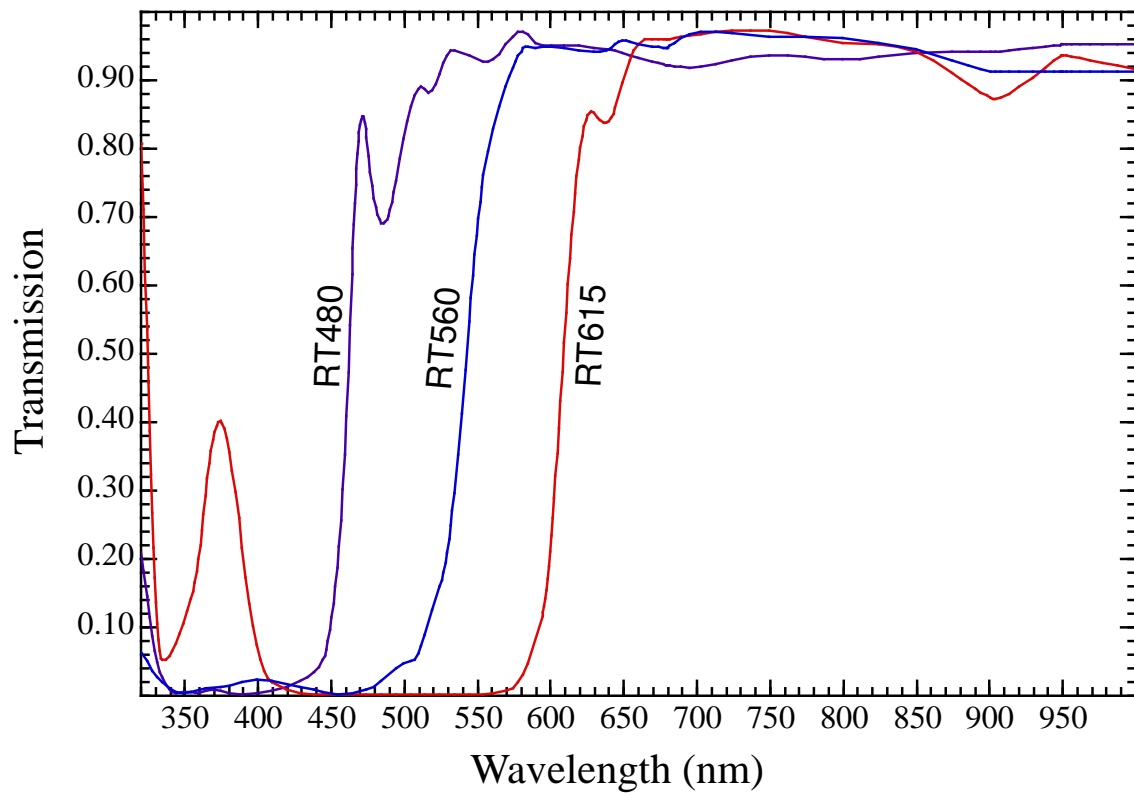


Fig. 9.— The transmission of the WiFeS dichroics. The reflectivity in the blue is assumed to be the complement of these curves.

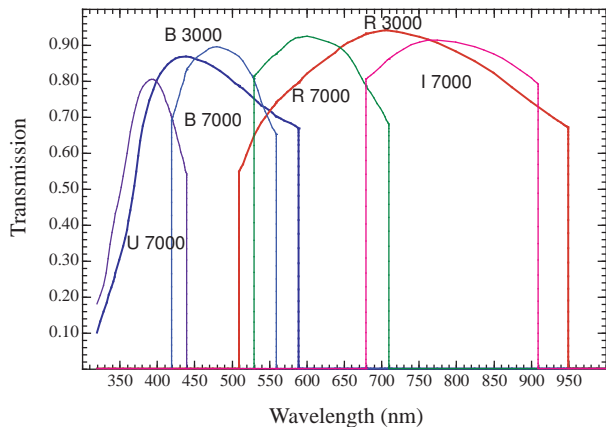


Fig. 10.— The grating efficiencies in their first order of the WiFeS gratings measured at their nominal operating angle of incidence. The efficiency is plotted only over the wavelength range for which each grating is intended to be used.

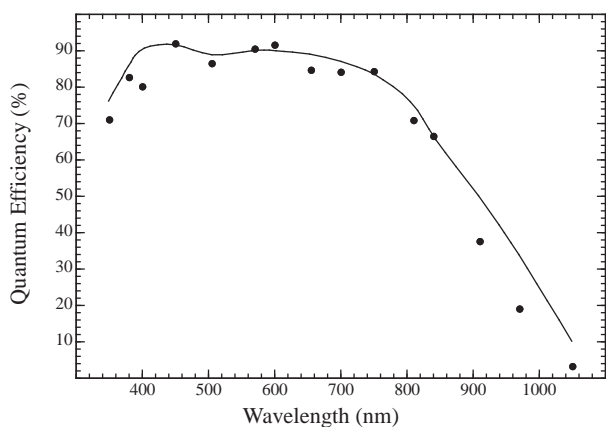


Fig. 11.— The measured QE of the Fairchild (blue QE enhanced) engineering test detector for WiFeS. The points are our laboratory measurements, which have an uncertainty comparable to the size of the spot, and the smooth curve shows the QE reported by the manufacturer. Note that the measured QE points fall below this curve in the red. This is a consequence of the cooling of the detector, which is necessary in order to reduce the dark noise to acceptable levels for our purpose.

salt water, acid and base tests, and hydrogen sulfide atmosphere. This coating delivers an average reflectivity greater than 95% from 300 to 2500nm, and a reflectivity $>99\%$ below 390nm. It uses over- and under-coats of NiCrN_x , nickel chromium nitride, for toughness and to retard diffusion. Layers of SiO_2 and Nb_2O_5 can be used to increase the reflectance at selected wavelengths. The coating can be washed with water, and wiped with a cloth, but it is stripped with sodium thiosulfate. Regrettably, these coatings are no longer available - the WiFeS mirrors were the final set to be produced by the LLNL facility.

The measured reflectivity of our mirrors is shown in Figure 8. This coating was used for both the image slicer and the collimator, the only mirror surfaces in the spectrograph. In addition, we manufactured a new Nasmyth tertiary for the 2.3m telescope, and had this coated with the same material, thus improving the throughput of the telescope by 3 – 19% compared with fresh aluminium. Together, these three mirrors provide 10 – 60% increase in system throughput compared with aluminium. These gains are especially valuable both in the UV, and in the $\sim 800\text{nm}$ absorption waveband of aluminium.

7.2 Dichroics

The WiFeS dichroics, supplied by Cascade Optics, are designed to provide maximum throughput when used with the correct gratings as shown in table 1. The dichroic cut then occurs in the unobserved wavelength band. The performance of the dichroics is shown in Figure 9. D3 is excellent, and D1 and D2 are very good. The blue leak apparent in these dichroics should not appreciably affect performance, since it lies largely out of band of the blue grating that will be used with them.

7.3 Gratings

All grating blanks are made of Ohara BSL7Y glass, which provides a high transmission below 340 nm. These were provided as 7 mm thick polished and figured substrates to the VPH grating manufacturer (ATHO²L of Liege), who then fabricated the grating and assembled the sandwich. The outside surfaces were then post polished and anti-reflection coated for optimum transmission and wavefront quality. The anti-reflection coatings are optimized for the particular wavebands, which should provide reflectivities of the order 0.5% per air-glass surface. For the low-dispersion mode, the anti-reflection coating is applied to the outside faces of the prisms, the internal face being bonded to the VPH grating sandwiches. For the prism, the beam is incident on

their outside faces at large angle. We therefore expect a poorer performance for the anti-reflection coatings; about 1.0%.

Figure 10 shows the result of laboratory tests of the gratings at the angle of incidence that they will be actually used (22° in the case of the high dispersion gratings). The measurements below 400 nm are unreliable. The UV performance is in any case, much lower than the manufacturer’s estimate in the U 7000 grating, and at the short wavelength end of the B 3000 grating. They measured the zeroth order throughput only, and the grating efficiency had to be estimated by assuming all the rest of the light was placed in the first order. Our measurements show that losses into the second order are quite important for the U 7000 and (to a lesser extent) the B 7000 gratings. Furthermore, the substrate transmission appears to be lower than expected, either due to gelatin of the grating, or the bonding glue. This is being further investigated.

The peak efficiency of these gratings can be maximized by tilting the grating to place the maximum throughput at the super-blaze angle. The effect of this was tested by repeating the grating efficiency measurements at a range of angles. All these gratings have the peak of their super-blaze within 3° of the nominal operating angle. Except for the U 7000 grating the peak efficiency is not more than 2 – 3% higher. For the U 7000 grating, the peak efficiency at the nominal operating angle is shifted to shorter wavelengths than the super-blaze peak, which provides improved efficiency at the shortest wavelengths.

All VPH gratings operated in Littrow will show a significant ghost of zeroth order undispersed light. This was described by Wynne et al. (1984) and Saunders et al. (2004). It is due to light reflected from the detector, recollimated by the camera, and reflected in $\pm 1^{\text{st}}$ order by the grating to form an undispersed beam which is reimaged by the camera onto the detector. This ghost will be present at low level on the WiFeS detectors. We have evaluated this from the point of view of theory, and we do not believe it will present a significant problem. However, this remains to be verified on-telescope during the functional verification testing.

7.4 Cameras

The cameras provide a transmission of better than 90% over most of the wavelength range of operation, and all air-glass surfaces have been anti-reflection coated to provide a reflection of $\leq 1\%$. In the near UV the transmission is limited by the thickness and type of glass materials used. The transmission falls to 80% at 360 nm, and to $< 40\%$ below 330 nm which represents the effective limit of operation of the spectrograph.

The multi-element lenses of the camera are coupled by UV-transmissive oil, and there is a small reservoir with a piston which allows for the differential thermal expansion of the elements. This opens and closes the gaps between the lenses, which the oil fills. The whole assembly is sealed with O-rings which are carefully selected so as to not leach UV-absorbing organic materials into the coupling oil.

One of the lenses is mounted on “thermal bellows” (Figure 12) which provides passive correction of the focal plane scale against thermal expansion of the camera optics. The bellows consist of invar rods screwed into a steel framework, and it converts thermal expansion into the appropriate translational movement of the lens cell which controls the f-ratio of the camera.

7.5 Detectors

The detectors are to be Fairchild 4096×4096 devices with $15 \mu\text{m}$ pixels. Each camera is to have a detector optimized for the wavelength of operation. Since the final scientific devices have not yet been delivered, we present results for a blue-sensitive engineering device. The quantum efficiency (QE) was measured at the RSAA detector lab on a monochromator against a standard Hamamatsu photodiode. The resulting QE curve is plotted in Figure 11. Low temperature operation of the chip reduces the QE in the red, as can be seen from these data.

In order to reduce the read-out time, we will operate these devices with dual-port readout. This will provide a readout time of $\sim 30\text{s}$.

The dark current and read-out noise of these devices is excellent. Data from 3600s dark exposures made at the operating temperature of -120C , and a system gain of $0.9\text{e}^- \text{adu}^{-1}$ and $0.89\text{e}^- \text{adu}^{-1}$ on the A-side and the B-side, respectively were analysed. These gave a net dark current of 6 and $5 \text{e}^- \text{Hr}^{-1}$ on the A-side and the B-side, respectively. The readout noise for these and for shorter exposures was $3.8 \text{e}^- \text{Hr}^{-1}$ for both readout ports. These figures are sufficiently low to ensure that the spectrograph will be sky-noise limited in its $R = 3000$ mode over most of the wavelengths of operation.

8 System Throughput

The end-to-end transmission expected for the WiFeS spectrograph is shown in Figure 13. In these calculations we have included the transmission of the atmosphere, the telescope, the de-rotator optics, the slicer and stacker, the spectrograph including the collimator, camera, gratings and dichroics and the detector performance. The primary and secondary are assumed to be

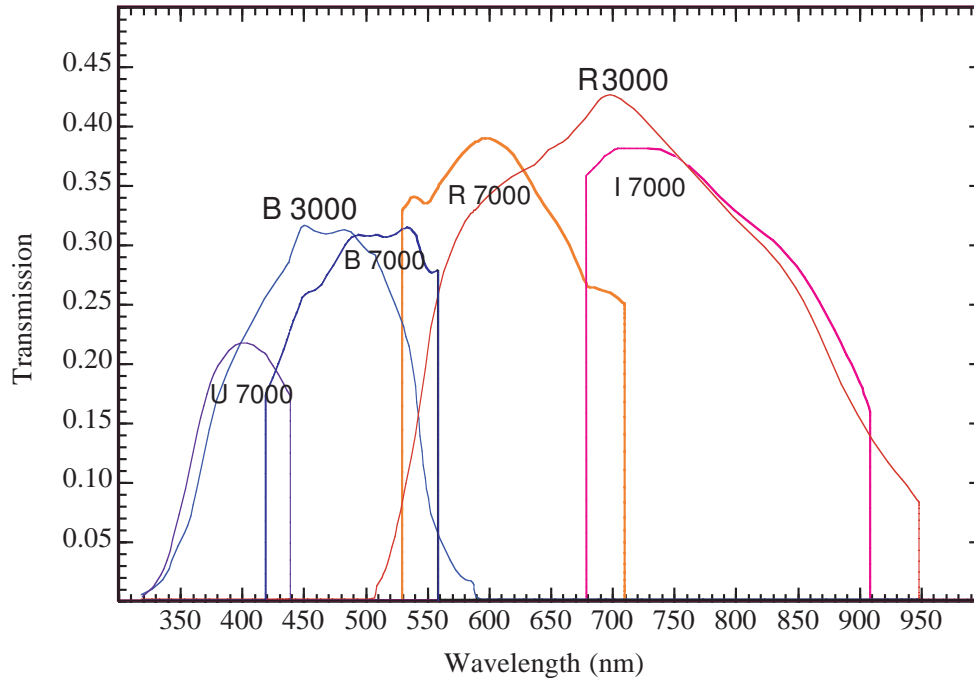


Fig. 13.— The computed on-telescope end-to-end transmission of WiFeS spectrograph, including the telescope, atmosphere and detectors for both the low dispersion $R = 3000$ modes and the high resolution $R = 7000$ modes. Note the generous overlap between the various wavebands. This is important in ensuring accurate spectrophotometry throughout the spectrum.

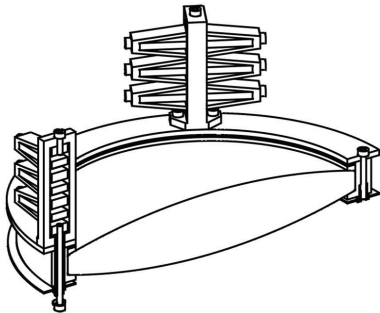


Fig. 12.— The “thermal bellows” mount which is used to provide passive correction of the focal plane scale against thermal expansion of the camera optics. The bellows consist of invar rods screwed into a steel framework, and it converts thermal expansion into the appropriate translational movement of the lens cell which controls the f-ratio of the camera.

uncoated Al. For the transmissive optics, all air-glass surfaces are assumed to be A/R coated, with a reflectivity of 1%. The bulk absorption coefficients of the various optical materials are taken from the literature.

The transmission of the instrument averages about 30% in the 4000-9000Å region, which clearly satisfies the science requirements for high throughput.

8.1 System Sensitivity

The effective end-to-end collecting area of WiFeS is 5000cm² (U), 15000cm² (B), 13000cm² (V), 18000cm² (R) and 5000 cm² (I). This implies a stellar photon count rate Å^{-1} at $V = 15$ of 4Hz (U), 21Hz (B), 13Hz (V), 11Hz (R) and 2 Hz (I). By comparison, the night sky count rate Å^{-1} at SSO in dark sky conditions is estimated to be 0.007 Hz (U), 0.017 Hz (B), 0.021 Hz (V), 0.043 Hz (R) and 0.040Hz (I). These translate to count rates per pixel on the detector at $R=3000$ of 0.003 Hz (U), 0.014 Hz (B), 0.019 Hz (V), 0.050 Hz (R) and 0.066 Hz (I).

WiFeS therefore becomes sky-limited at 22.0 (U), 22.7 (B), 22.0 (V), 21.1 (R), and 19.2 (I), provided that the dark current and readout noise in the detectors is below $\sim 0.01 \text{ Hz pixel}^{-1}$. This is a pessimistic estimate, since these sources of detector noise have been

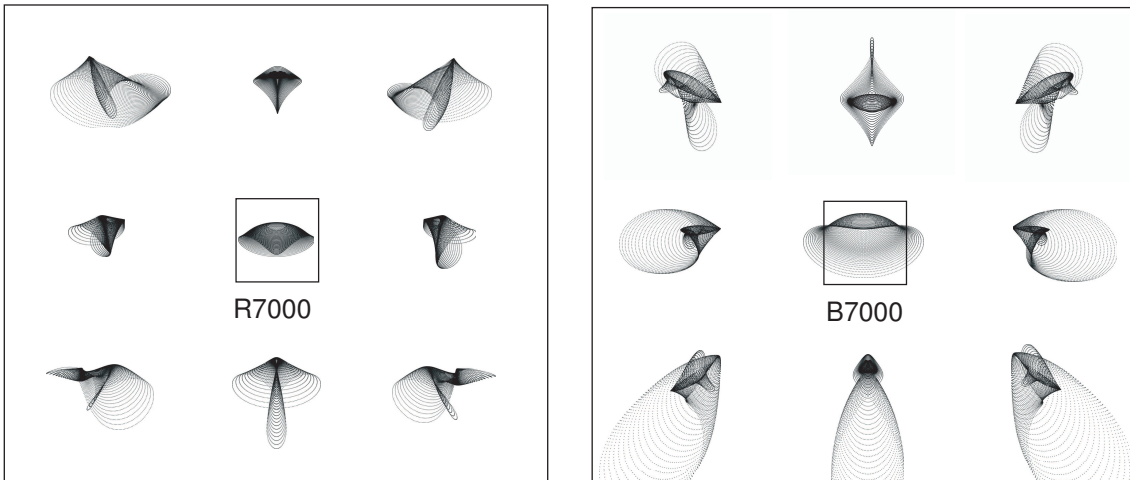


Fig. 14.— The computed end-to-end image quality of WiFeS with the R7000 and B7000 gratings. The small box represents 2 pixels on the detector ($30\mu\text{m}$ square). The nine spot diagrams for each grating correspond to positions at the centre of the science field, at each corner, and in the middle of each side.

measured at $\sim 0.003 \text{ Hz pixel}^{-1}$ for the engineering device.

For a 22 mag star (at all wavebands), and under seeing conditions ~ 1.0 arc sec., the exposure time needed to provide sky-limited exposures with a S/N=10 per resolution element in the $R = 3000$ mode is of order 7Hr (U), 1.2Hr (B), 1.4Hr (V), 1.6Hr (R) and 4.4Hr (I). Thus, the effective limiting magnitude in the $R = 3000$ mode is 22 mag, or perhaps a little fainter. For extended sources we estimate an effective limiting surface brightness of $\sim 10^{-17} \text{ erg cm}^{-2} \text{ arcsec}^{-2} \text{ s}^{-1} \text{ \AA}^{-1}$ in the $R = 3000$ mode.

9 Image Quality

The typical seeing expected at Siding Spring is $\sim 1.0 - 2.0$ arc sec. To maximize the Felgett advantage, the instrument should be capable of using the periods of best seeing effectively, but it should not over-sample the point spread function. This requirement drives the goals of the optics design; both to match the image performance of the camera and spectrograph to the slitlet width at the detector (2 pixels or 1.0 arc sec. on the sky) and to provide one spectral and spatial resolution element for 2 pixels on the detector.

The optical performance is limited largely by the cameras and to a lesser extent by the uncorrected collimator, which is operated slightly off-axis. The cameras are fast (F-2.6) and must operate of a wavelength range that is quite demanding. The collimator is made as fast as possible (F-12) to minimise the overall instrument

length and weight. The collimator produces off-axis spherical aberration that appears as astigmatism.

The end-to-end image quality for the fore-optics, image slicer, spectrograph and camera is given in Figure 14. Here, we show both the best and the worst image quality within the field covered by the detector. In general, these correspond to a point close to the centre and a point at an extreme of wavelength near the edge of the field, but these points differ between the various gratings.

In order to avoid degrading the spectral resolution, our objective was to ensure that the slit width is matched to 2 pixels on the detector, and that the ensquared energy is everywhere less than, or at worst equal to this projected slit width. This requires that 70% of the encircled energy be placed within $15\mu\text{m}$ on the detector. The computed best and worst ensquared energies are shown in Figure 15.

Camera aberration is highly dependent on field position. Collimator aberration is independent of field position because of the concentric nature of the IFU. In some cases the collimator and camera aberrations counteract to improve image quality. It is clear that the overall image quality and hence the spectral resolution are remarkably uniform throughout the field. This is a great advantage in interpreting the reduced WiFeS data.

10 Summary

The WiFeS instrument is an integral field spectrograph offering unprecedented performance and field coverage.

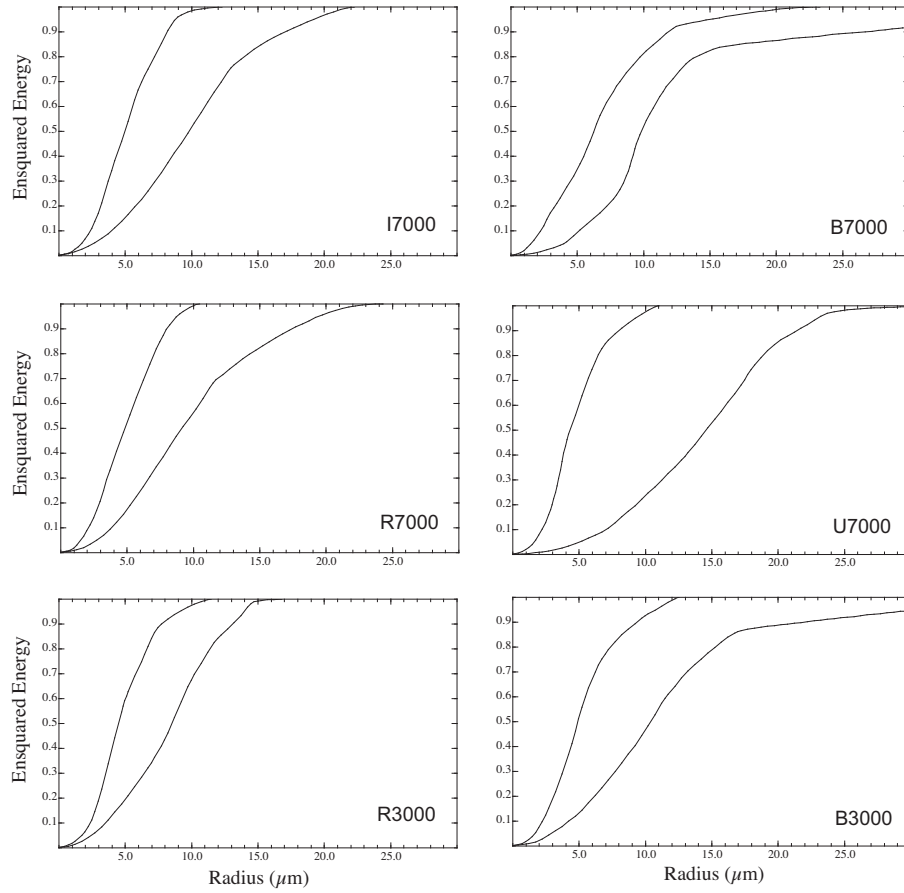


Fig. 15.— The ensquared energy performance of WiFeS for each grating. The two curves are for the best and for the worst image quality within the whole of the science field. The design goal was to place at least 70% within $15\mu\text{m}$ on the detector so that the resolution is set by the width of the entrance slit. This goal is met at all wavelengths except at the short-wavelength end of the U 7000 grating; below 350 nm where the optical design proceeded on a ‘best effort’ basis only.

It maximizes the number of spectral elements (a total of 4096 independent elements per exposure), and the reflective image slicing design maximizes the number of spatial elements by matching spatial scale of the image at the detector to the expected seeing. WiFeS has a science field shape (25x38 arc sec) which is well-matched to typical spatially extended science targets. With the typical ~ 1.0 arc sec seeing expected at Siding Spring, it presents 950 independent spatial elements.

The scientific performance of the spectrograph has been maximized through:

- A reflective image slicing which ensures good spectrophotometric characteristics.
- A stationary spectrograph body. This eliminates flexure, and provides a stable thermal environment, ensuring that the wavelength calibration remains fixed and stable.
- Maximization of the throughput to maximize scientific productivity.
- Provision of an “interleaved nod and shuffle” mode. This allows photon noise-limited sky subtraction, and permits the observer to both see and to evaluate the sky-subtracted data at the telescope.
- Fixed modes of operation, with all gratings and dichroics mounted within the spectrograph body. This allows rapid changes in instrumental configuration, the progressive building up of calibration libraries, and efficient batch-mode data reduction.
- A design which is very well baffled against scattered light, and which has very low ghost image intensity, ensuring that fields with very large luminance contrast can be effectively observed.

WiFeS will provide resolutions of $R = 3000$ (100 km s⁻¹) and $R = 7000$ (45 km s⁻¹) throughout the optical waveband, to a limiting magnitude of ~ 22 for stellar sources, and $\sim 10^{-17}$ erg cm⁻² arcsec⁻² s⁻¹ Å⁻¹ for extended sources. With these performance figures, WiFeS will be highly competitive with spectrographs operating on much larger telescopes.

Acknowledgements The authors of this paper acknowledge the receipt of the Australian Department of Science and Education (DEST) Systemic Infrastructure Initiative grant which provided the major funding for this project. They also acknowledge the receipt of an Australian Research Council (ARC) Large Equipment Infrastructure Fund (LIEF) grant LE0775546, which allowed the construction of the blue camera and associated detector module.

References

- Arribas, S. & Mediavilla, E. 2000, in *Imaging the Universe in Three Dimensions* eds W. van Breugel & J. Bland-Hawthorn, *ASP Conference Series*, 195, 295
- Bacon, R. et al., 2001, MNRAS326, 23
- Content, R. 2000, in *Imaging the Universe in Three Dimensions* eds W. van Breugel & J. Bland-Hawthorn, *ASP Conference Series*, 195, 518.
- Cuillandre, J. C. et al., 1994, A&A, 281,197
- Glazebrook, K.. & Bland-Hawthorn, J. 2001, PASP, 113, 197
- McGregor, P. J., Conroy, P., Bloxham, G. & van Harmelen, J. 1999, PASA, 16, 273.
- McGregor, P. J., Dopita, M. A., Wood, P. & Burton, M. G. 2001, PASA18, 41
- McGregor, P. J. et al. 2003, in *Instrument Design and Performance for Optical/Infrared Ground-based Telescopes*, M. Iye & A. F. M. Moorwood, eds., Proc. SPIE, 4841, 1581
- McGregor, P. J., Dopita, M. A., Sutherland & Beck, T. 2007, Ap&SS, in press.
- Jaquinot, P. 1960, Rept. Progr. Phys. 23, 267
- Rodgers, A. W., Conroy, P. & Bloxham, G. 1988, PASP, 100, 626
- Roth, M. M. et al. 2000, in *Imaging the Universe in Three Dimensions* eds W. van Breugel & J. Bland-Hawthorn, *ASP Conference Series*, 195, 5810
- Saunders, W. Bridges, T. J., Gillingham, P., Haynes, R. & Smith, G. A. 2004, Proc. SPIE, 5492, 146
- Thomas, N. L., Wolfe, J. & Farmer, J. C. 1998, Proc. SPIE, 3352, 580
- Tinney, C. G. 2000, in *Imaging the Universe in Three Dimensions* eds W. van Breugel & J. Bland-Hawthorn, *ASP Conference Series*, 195, 100
- Wolfe, J. & Sanders, D. 2004, “Optical & Environmental Performance of Durable Silver Mirror Coatings Fabricated at LLNL”, paper presented to the mirror days at Hunsville, Alabama, 2004, available at URL: optics.nasa.gov/tech_days/tech_days_2004/docs/Document_21.
- Wynne, C. G., Worswick, S. P., Lowne, C. M., & Jorden, P. R. 1984, in *Notes from Observatories (RGO)*, 104, 23.

11 WiFeS Observing

11.1 Getting Started under CICADA

Until the TAROS system is fully installed, observers will have to observe under a CICADA lash-up. This section describes the procedures which must be used under the CICADA control system.

The essential data for WiFeS observing is to be found on:

http://www.mso.anu.edu.au/observing/ssowiki/index.php/WiFeS_Main_Page.

This page includes a performance calculator written by Peter McGregor, which facilitates the preparation of the observations. An example of the interface and output is give in Fig (16).

In setting up for observing the observer should be aware that the nominal focus positions of the cameras are at:

-1 (Red) and
+7 (Blue).

Both cameras are temperature compensated, so it should not be necessary to change these during an observing run.

In its final configuration WiFeS will operate under TAROS (Telescope and Remote Operating System). The operation and interface of this system is given in the following section. However as of April 2009, this is not yet implemented and the observer must use the Cicada system. In this mode, the guiding is done through the *Maxim* system in a Windows terminal. The observer login password for this computer is *guyer*.

To run the Cicada system at the 2.3m telescope, you must first log in under your username and password. For those without an ANU account, contact the system administrator on:

`sysman@mso.anu.edu.au`

Then type:

```
> ssh missus
> cicada &
```

11.2 In case of CICADA Crash

If you get errors, a crash or a system freeze up you need to type:

```
> sudo /opt/cicada/wifes_cleanup
```

and then restart Cicada. To display your spectra at the telescope use:

```
> ds9 &
```

On startup after a crash, it may become necessary to "home" the mechanisms. These are controlled by absolute encoders, so it should not be necessary to do this. However, the homing routines ensures that a mechanism drive is really where it thinks that it is. In case you need to rehome in the small hours. The commands you'll need to run (on missus only) are:

```
> sudo /opt/cicada/make_wifes_home
```

This will change the cicada configuration to make WiFeS home on a Cicada restart (*i.e.* stop Cicada, if it is running, run this command and then restart Cicada). Homing takes up to 10 minutes, and no instrument mechanism drives can be run if this is going on. To reverse the effect of this command run:

```
.> sudo /opt/cicada/make_wifes_not_home
```

11.3 Additional Advice

The detectors are read out in quad-readout mode. Thus, all Bias frames are divided into quadrants with slightly different levels in each. If the mis-match between quadrants is too great, this can be rectified by a technician. Readout of the chip in quad-readout mode takes 90 sec, so be patient while this happens, and think of all the lovely data you are getting.

Try not to abort exposures. This regularly causes Cicada to freeze or to crash.

All WiFeS mechanisms are controlled through a Galil controller which is in the electronics rack next to the instrument. The normal operating state should show two sets of two green LEDs with a flashing yellow on under each pair. In case that red lights are showing, note which these are, and call a technician.

The observer should also check that the float valve in the dry air supply line is functioning normally. Just one ball should be floating, and the gas flow rate should be in the range 5 -10 cc/s. Too strong a gas flow will cause the WiFeS shutter to jam due to over pressure in the instrument. The symptom of a shutter jam is that the intensity of the illumination is much reduced, and there is pronounced vertical streaking visible in any images obtained in this condition.

The observer should also check the coolant lines to the (gold coloured) CCD controllers. There should be

WiFeS Performance Calculator

Parameters		Results	
Exposure: <input type="text" value="1200"/> sec; cycles <input type="text" value="3"/>		Adopted integration time s <input type="text" value="1200"/>	
Sky: <input type="text" value="0000-0000-0000-0000-0000-0000-0000-0000-0000-0000"/>		Adopted cycles <input type="text" value="3"/>	
<input type="checkbox"/> Integration time <input type="text" value="1200"/> sec; cycles <input type="text" value="3"/>	Moon phase <input type="text" value="000"/>	Star signal e ⁻ /pix <input type="text" value="31"/>	
<input checked="" type="checkbox"/> Star brightness <input type="text" value="20.0"/> mag	Seeing FWHM <input type="text" value="1.0"/> arcsec	Galaxy signal e ⁻ /pix <input type="text" value="0"/>	
<input type="checkbox"/> Galaxy brightness <input type="text" value=""/> mag/arcsec ²	Airmass <input type="text" value="1.0"/>	Line signal e ⁻ /pix <input type="text" value="0"/>	
<input type="checkbox"/> Line brightness <input type="text" value=""/> erg/s/cm ² /arcsec ²	Spectrograph: <input type="text" value="0000-0000-0000-0000-0000-0000-0000-0000-0000-0000"/>	Sky signal e ⁻ /pix <input type="text" value="3"/>	
<input type="checkbox"/> Line FWHM <input type="text" value=""/> km/s	Grating <input type="text" value="0000-0000-0000-0000-0000-0000-0000-0000-0000-0000"/>	Dark signal e ⁻ /pix <input type="text" value="2"/>	
Objective: Star <input checked="" type="radio"/> Galaxy <input type="radio"/> Line <input type="radio"/>	Read noise <input type="text" value="4.1"/> e ⁻	Total signal e ⁻ /pix <input type="text" value="36"/>	
<input type="button" value="RESET"/> <input type="button" value="CALCULATE"/> <input type="button" value="HELP"/>		Total noise e ⁻ /pix <input type="text" value="7.3"/>	
		Signal-to-noise ratio /aperture <input type="text" value="10.44"/>	

This tool models the performance of the [Wide-Field Spectrograph \(WiFeS\)](#).
 Peter McGregor (peter@mso.anu.edu.au) | Access no. / Last updated May 15, 2008.
 Research School of Astronomy and Astrophysics, College of Science, The Australian National University.

Fig. 16.— A sample of the output from the performance calculator.

no leakage of coolant from these or from the coolant manifold. If there is, call a technician.

Never touch the detector Dewars or the silver braided cooling lines running into them which come from the Cryo-Tiger cooler. **The detectors can be destroyed by static electrical discharge from the observer's hand. The cooling lines are under the maximum load permitted. Rupturing the gas seal on the cooling lines will cause highly flammable gases to escape, with consequent risk of catastrophic explosion.**

12 The WiFeS Observation Sequence Window

Under TAROS, the WiFeS Telescope Control System (TCS) interface is shown in Fig (17). It is divided into several main sections:

- **Observation Sequence Setup:** This refers to the various observational modes which may be chosen, *see* Section (11), below. The standard mode is *Classical Equal*, but modes of *Classical Unequal*, *Node and Shuffle* and *Subaperture nod and shuffle* may also be selected. For the latter case, the *Secondary Beam Centre* field is disabled, and displays “Slit offset 19 arc sec.”. The *Master Camera* mode is activated when we are making un-equal exposures in the different cameras. The master camera is the one making the short exposures. The number of exposures is set in the *No. of Sequences* window. The number of sub-exposures or nod and shuffle cycles is set in the last window. The label changes according to the mode.
- **Filter and Arc Setup:** Here we can choose filters, lamps and arcs. When the arc mirror is in the arcs are enabled. Neutral density filters can be selected in the main beam. This may be useful for bright star acquisition using the *Field Viewing Camera*. The choices are NG9 (a glass filter, UV transmission poor), and reflective coated 0.01%, 0.1%, 1.0%, and 10% filters. These filters are not calibrated. The choice of arcs is: QI-1 (Quartz iodine lamp), Ne-Ar, Cu-Ar, QI-2 (currently a QI lamp, but we are hoping to replace this with a Deuterium lamp to provide a flat-field UV continuum for the U7000 and B3000 gratings. The arc neutral density filter attenuates the strength of the arc. The control button will be set up to jog mode with the number of steps to jog being set up in the GUI.
- **Components Setup:** Here we choose which dichroic to use, where the aperture wheel is set and which gratings we are using. The standard combinations of dichroics & gratings are RT480 + U7000 + R7000; RT615 + B7000 + I7000, RT560 + B3000 + R3000 and RT560 + B7000 + R7000. Other combinations *e.g* RT480+U7000+R3000 are also possible, but the calibrations for these may not exist in the library.
- **Assign Beam:** Here we set up the pointing coordinates for the observation. Normally these will be *Beam A*: The coordinates of the object to be observed. This will be usually the one for

which guiding is used, so the guide box should be checked. *Beam B*: The coordinates of the sky background reference. This will be used in the *Classical Equal*, *Classical Unequal*, and *Node and Shuffle* modes. For the *Subaperture nod and shuffle* mode, set the coordinates of the object up, and the telescope will automatically set up the offset coordinates for you (*see* Section 11 and fig 18).

- **Instrument Indicators:** In this window the camera and CCD temperatures are given and the read-out or expose status is displayed at all times.
- **Instrument State:** Displays the state of motion or position of all key optical components. These will move only when an *Expose* command has been implemented.
- **Observing Block Status:** In this window the progress of TCS scripts to perform a sequence of exposures is displayed.

There are two other tabs visible in Fig (17). The first of these labelled **Quick-Look Image Display** allows the observer to inspect the raw data and the sky-subtracted data (obtained when the nod and shuffle mode is in use). The latter image is formed by moving the first image by 80 pixels with respect to itself, and subtracting it from itself.

The second tab labelled **Field Viewing Camera** allows one to set up exposures of the below-aperture field viewing camera. This camera directly sees what is being projected onto the image slicer, and so can be used to set up the instrument, or can be used in both acquisition and re-acquisition of faint targets. When the number of exposures and the exposure time has been set up, the command *Expose* will operate the flip mirror or (**Interceptor**) which comes into the beam above the slicer, and reflects the image into the field viewing camera. The camera read-out or expose status is displayed at all times. When a normal WiFeS exposure is activated, the flip mirror is automatically removed from the beam.

Note: The configuration of the spectrograph, the arcs *etc.* is not set until the observer hits **Expose**. The commands are then sent to the TCS and the mechanisms which need to be activated are then driven. As a consequence, the observer may note a delay before the exposure actually starts. This is normal. The progress of the set-up can be monitored in the *Instrument State* sub-window.

13 Acquisition & Guiding

Since the WiFeS spectrograph is mounted at the Nasymth focus of the RSAA 2.3 m telescope, it does

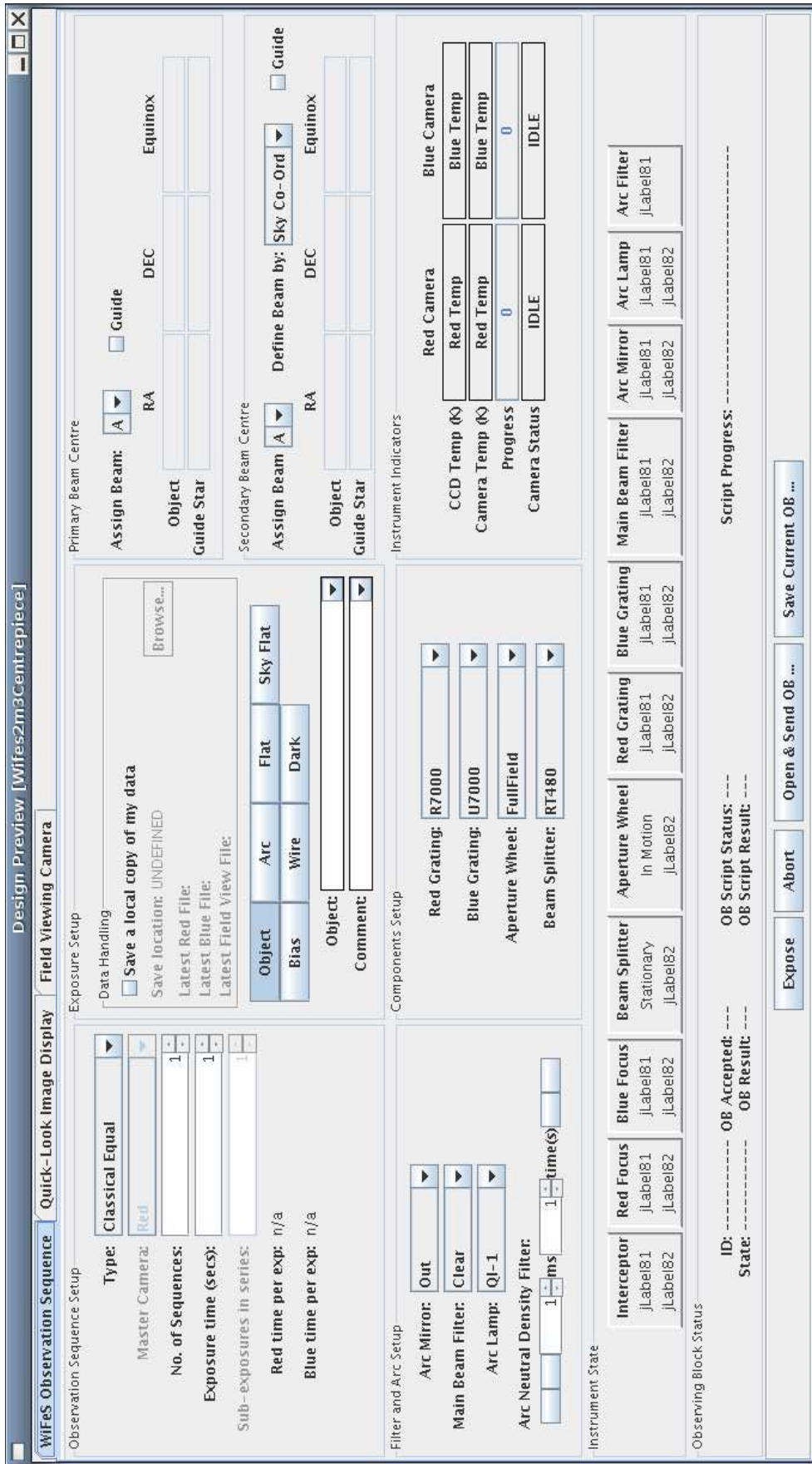


Fig. 17.— The WiFeS Observation Sequence Window.

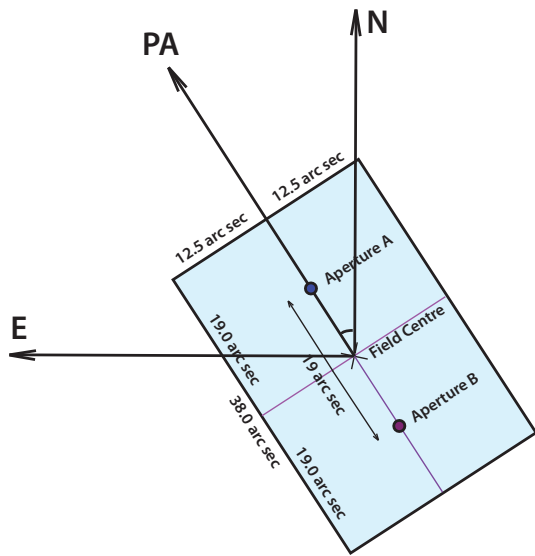


Fig. 18.— The definition of the coordinate system used by WiFeS. For pointed observations, the object is placed upon the field centre as shown. The position angle is measured along the central slice. For sub-aperture nod-and-shuffle observations (*see below*, the observer sets up the notational coordinates to the centre of the field. When the sub-aperture nod and shuffle is selected, the telescope control system will define the apertures A (object) and B (sky) automatically, and will start the observing sequence in position A.

not rotate, so field rotation is dealt with by placing an instrument field mask at the f/18 focus, which rotates with the telescope field, followed by a de-rotator and relay optics which projects the field mask onto the (fixed) image slicer. The field mask will accept a field size of approx 25 x 38 arc second, and this maps to the 25 slices each 1.0 arc sec wide x 38 arc second long at the image slicer.

These instrumental characteristics affect the image acquisition, re-acquisition and guide strategies that need to be employed, and these strategies and the science acquisition modes that might be employed by observers are described here.

The coordinate system used by the WiFeS instrument is given in fig 18.

13.1 Pre-observing set up

The following pre-observing set up is common to all acquisition and guide modes:

1. Rotate a 0.5 arc sec pinhole aperture mask into the beam, and diffusely illuminate it with continuum source so that it acts as an artificial star.
2. Insert the field viewing camera mirror located above the image slicer, and adjust focus if necessary. Note the coordinates of artificial guide star in the field viewing acquisition camera. *Note:* The focal plane scale of this camera is the same as for the slicer; 0.5 arc sec. per pixel.
3. Move the telescope to various points on the sky (in track mode) to ensure that coordinates of artificial guide star do not shift. If they do, this means that there is an error in the de-rotator prism axis. If this is too great (≥ 1.0 arc sec on the sky), the de-rotator prism may need re-aligning. Report if this condition is encountered.
4. If the coordinate shift is acceptable (< 1.0 arc sec on the sky), field viewing acquisition camera mirror, and take a test exposure to discover whether the artificial guide star is centred on the central slice of the image slicer. If not, and if the observer wants proper centering of the star for single-star observations, then the telescope rotation axis may need to be re-defined (see below).

13.2 Basic Acquisition

The WiFeS science aperture produces a large hole in the observing field. It is therefore better to perform

the initial acquisition in a different part of the acquisition camera, and then to move the object to be observed into the WiFeS science aperture. For this, we suggest that you use the:

> define aperture

command of the TCS (telescope control system). This activates an interactive sequence, described in the TCS handbook. The recommended sequence is as follows:

- Point at a rich star field, such as a globular cluster. Take a long-exposure image while rotating the rotator. This establishes the centre of the field rotation. Mark it.
- Choose a convenient star of known coordinates. This can be done by issuing the TCS command:

> track file stars10

The star can be chosen by opening the `stars10` file under the tab “Files” in the TCS window. If, say, star 39 is chosen, issue the command:

> track 39

- Centre the star the star at the centre of field rotation. Issue the command:

> calibrate aperture B

and follow the interactive instructions.

- Move the star to the centre of the WiFeS aperture. It may be centered using the field viewing camera with the coronagraphic aperture. Now issue the command

> calibrate aperture A

and follow the interactive instructions.

- Move the star back to aperture B using the command:

> aperture B

centre up, and issue the command:

> calibrate pointing

- The telescope is now set up to acquire your science object in aperture B. When you have centered it,

simply issue the command:

> aperture A

and choose a guide star. The object is now centred in the WiFeS science aperture.

This procedure will be adequate to acquire most science objects to sufficient accuracy. If greater accuracy is required, follow the more sophisticated procedures mapped out in the following sections.

13.3 Bright Point Source Acquisition

For bright point sources, we need to acquire and to keep the source centered on the same point of the image slicer, so that the spectrum is always found on the same columns of the detector. Since the image spread may exceed 1.0 arc sec, under conditions of poor seeing, the observer will need to use a larger extraction aperture, which is equivalent to extracting the stellar data from the slices adjacent to the central one, and then combining the data from all three slices to form the final spectrum. For bright point sources (stars), the following acquisition procedure will be used:

1. Rotate the coronagraphic science aperture into the beam, and use field viewing acquisition camera to centre the star in this aperture in the middle of the wire. Use the coordinates of the star to define the telescope rotation axis and telescope pointing.
2. Exchange the coronagraphic science aperture for the full-field aperture, and confirm that the star is still properly centred. Record the star pixel coordinates on the camera focal plane.
3. Choose an offset guide star and set up for auto-guiding in the acquisition and guide camera.
4. Remove the field viewing camera mirror located above the image slicer, and start your exposure.
5. Repeat steps 2 to 4 as necessary, with a frequency which depends on the drift of the source with time, which in turn depends on the PA and ZD of the observation. The drift is determined by misalignment of the de-rotator prism, and by changing atmospheric refraction as a function of zenith distance. Typically you might choose to repeat a guide cycle every 30 min or only every 60 mins.

13.4 Faint Point Source Acquisition

Faint point sources may not be visible in either of the acquisition cameras. In this case, the following acquisition procedure will be used:

1. Rotate the coronagraphic science aperture into the beam, and use field viewing acquisition camera to centre a nearby bright acquisition star of known coordinates in this aperture (in the middle of the wire). Use the known coordinates of the star to define the telescope rotation axis and telescope pointing.
2. Exchange the coronagraphic science aperture for the full-field aperture, and confirm that the star is still properly centred. Record the star pixel coordinates on the camera focal plane.
3. Remove the field viewing camera mirror located above the image slicer.
4. Feed in the coordinates of the target object and slew the telescope to these coordinates.
5. Inspect the guide field, choose an offset guide star, and commence guiding.
6. Start your exposure.
7. Repeat steps 2 to 6 as necessary, with a frequency which depends on the drift of the source with time, which in turn depends on the PA and ZD of the observation. The drift is determined by misalignment of the de-rotator prism, and by changing atmospheric refraction as a function of zenith distance. Typically you might choose to repeat a guide cycle every 30 min or only every 60 mins.

13.5 Extended Source Acquisition

The acquisition and guide strategies that would be employed here depend upon whether:

1. The source has a bright nucleus, as would be the case for a bright galaxy or a galaxy with an active nucleus, or in the case of a planetary nebula or HII region with a central star, *or*
2. it is amorphous, or too faint to see in the acquisition cameras.

In case (1), the acquisition and guide procedures are identical to those for bright point sources (Section 12.3).

In case (2), the acquisition and guide procedures are identical to those for faint point sources (Section 12.4)

14 Data Accumulation Modes

There are two principal data accumulation modes:

1. “**Classical Mode**”, in which the data is accumulated in the red and/or blue cameras for a given exposure time *and*
2. “**Nod-and-Shuffle Mode**”, in which both object and nearby sky-background data is accumulated on the CCD chips in the red and/or blue cameras for a given (on-source) exposure time. In this case the actual observation time is twice the on-source exposure time plus the overheads associated with manipulating the shutter, nodding the telescope and shuffling the charge on the chip. However, these factor of two expose time overhead can be eliminated when the object covers less than 25x19 arc sec on the sky, and the observer can perform the variant of nod-and shuffle called “**Sub-Aperture Nod-and-Shuffle**”. This is described below.

14.1 Classical Mode with Equal Exposures

This is the simplest mode of operation in which shutter is opened for a given exposure time in both cameras, and then the accumulated charge on the CCD is read out in the normal manner. The total observation time is then the sum of the expose time plus the readout time – which is approximately 45 sec.

14.2 Classical Mode with Unequal Exposures

In *CICADA* the red and the blue camera controls are set up so that **red** camera is the “**master**”, while the **blue** camera is the “**slave**”. This assumes that the shorter exposures will generally made be with the **red** camera, so this camera needs to control the exposure sequence.

When an object is much brighter in either the blue or red (usually the red), or where there is a very bright emission line in either the blue or the red (usually red for arcs, but sometimes blue for objects), and one wishes to achieve high dynamic range so that both this bright line can be measured without saturation along with much fainter lines or a faint continuum, then the observer might choose to split up the exposure with the bright line or continuum between a number of shorter sub-exposures, while continuing with a single exposure with the other camera. In this mode the observational sequence is as follows:

1. Open shutter, expose for x seconds.

2. Close shutter, read out CCD with short sub-exposure and save file.
3. Repeat steps (1) and (2) up to (say) 8 times.
4. On last cycle (cycle N), read out both CCDs and save files.

We now have one exposure (of Nx seconds on-target exposure time) recorded in one arm, and N sub-exposures, each of x seconds on-target exposure time recorded for the other arm. The total observational time will be $(Nx + Nr)$ sec, where r is the read-out time (about 90 sec). This total observational time will be limited to about 60 min by dark current and cosmic ray considerations. Therefore, for 10 sub-exposures, each would have to be no longer than about 240 sec, giving an maximum observational efficiency of 66% in this mode. For 5 sub-exposures each of 5 sec the efficiency would fall to only 5%, which is clearly unacceptable. Since the read-out time is of order 90 sec, observational efficiency considerations limit the minimum sub-exposure time to a similar length of time. With two sub-exposures, the minimum observation time will be of order 4 mins on an astronomical object, but may be shorter for wavelength calibration arcs.

14.3 Nod-and-Shuffle Mode with Equal Exposures

This is the standard mode of nod-and-shuffle observing, and will most likely will be used in the majority of observations of faint objects. In this mode the sequence used by the telescope control system (TCS) and the *CICADA* software working together is as follows:

1. Once the object has been acquired, open the shutter and expose for x secs.
2. Close the shutter, shuffle the charge by 80 pixels to place the charge in the un-illuminated space between the images of the slitlets.
3. Suspend the guiding on the offset guide star.
4. Nod the telescope to new coordinates chosen by the observer which places the entrance slot on a relatively empty region of sky which can be used for sky reference.
5. Open the shutter and expose for z sec.
6. Close the shutter, shuffle the charge back by the same number of pixels, in order to return the signal accumulated on the object to its original position on the CCD.

7. Nod the telescope back to the nominal coordinates of the object.
8. Re-activate the guiding on the offset guide star, and wait for two guide cycles to ensure that the coordinates of the entrance slit have settled back to their original position.
9. Repeat steps (1) to (8) for $N - 1$ cycles.
10. Read out both CCDs and store the images.
11. Present to the observer the image of unshifted CCD image \ominus CCD image shifted by 80 pixels, and scaled so as to present only a restricted range around zero, so that the observer can see the sky-subtracted spectra of his or her faint objects.

Not counting the acquisition time, the total observation time will be $(2Nx + 2Nt + Na + r)$ sec. and the effective on-object exposure time will be Nx sec., where x is the exposure time in the individual sub-exposures, t is the telescope nod time, a is the guide star re-acquisition time and r is the CCD readout time. Typical values for an observation could be $N = 10$, $x = 150$, $t = 3$, $a = 6$, and $r = 90$, giving a total (on object) observation time of 1500 sec, a total observation time of 3170 sec and an observational efficiency of 47%. This might seem low, but this is compensated by the very high quality of the sky subtraction. This enables many such observations to be co-added with shot-noise image statistics.

In some cases, observers will use blank-field searches for very faint objects such as Lyman Break objects at redshifts greater than $z = 2$. In this case, both fields contain sky as well as the searched-for objects. Objects appearing in the “object” aperture will appear as positive signals in sky-subtracted images, and objects appearing in the “sky” aperture will give negative signals, thus allowing one to be distinguished from the other.

14.4 Sub-Aperture Nod-and-Shuffle

This mode is the recommended one for **Bright Star** observing. It is functionally indistinguishable from the previous nod-and shuffle mode with equal exposures (section 13.3). It will be used in the case that we are dealing with a single bright point source (star) in the field of view, or in the case where we are dealing with objects such as distant galaxies in which the object does not fill more than half of the WiFeS aperture (25×19 arc sec.).

In this case, we would organize that the star or galaxy is centered in the middle of one half of the galaxy (at an offset of 13;9.5 arc sec. from a chosen

corner of the WiFeS field. We would then arrange to nod the telescope along the long axis of the WiFeS field so as to place the star at field coordinates 13;28.5 arc sec. following nod. This has the advantage that the object is always in the aperture while the CCD is being exposed, giving an effective on-target efficiency of $2Nx/(2Nx+2Nt+Na+r)$. This doubles the efficiency, (to 93.4% using the figures given in the example given in the previous section (13.3).

In the extracted (sky-subtracted) image, we would have to extract a (positive) signal at 13;9.5 arc sec. from a corner of the WiFeS field, and a (negative) signal from coordinates 13;28.5 arc sec., and then add the moduli of these signals.

15 Calibration of Data

The following three subsections give the procedures to be followed in order that the data reduction pipeline can operate correctly. If absolute sensitivity calibration is required, then the spectrophotometric and black-body standards need also to be observed. However, even if these are not observed, a fairly good calibration can always be obtained from the calibration library, which will be progressively updated. This is particularly important for the reduction of *targets of opportunity*, for which it is assumed that the associated calibration frames will be generally incomplete.

15.1 Flat-Field Calibration

This part of the calibration should be carried out during the day, or in the evening before observing. First, illuminate the **Science Aperture** with a quartz iodide (QI) lamp. The illumination may either come from the calibration lamps located in the old DBS part of the instrument, located on the instrument rotator, or by the ring of QI lamps located on telescope top-ring and controlled by a wall switch outside the observers control room. These top-end ring lamps give a better illumination for flat field purposes.

If the telescope top-ring QI lamps are used, be sure to extinguish all fluorescent and incandescent lamps in the dome, and place a *Do not Enter: Flat Field in Progress* notice on the main entrance to the dome. Both the placement of the science aperture and the quality of its illumination can be checked using the field viewing acquisition camera, if necessary. However, recall that the CCD response in the viewing acquisition camera is not very even.

1. Take a series of bias exposures for use throughout the night.
2. Obtain three flat field images to a maximum exposure of $\sim 50,000$ counts per pixel for each combination of dichroic and gratings that are likely to be used during the night's observing.

Note: There may be an issue with the number of counts in the UV being too low. This will be examined during commissioning.

15.2 Aperture Calibration

Rotate the **Coronagraphic Aperture** into the beam, and repeat the set of quartz lamp exposures taken in Section 14.1. In these, the only difference will be the presence of a dark line down the centre of each slit spectrum. This provides the line which defines the slit

centre for each of the slices. These exposures may be referred to as the “**Wire**” exposure, to distinguish them from the “**Flat**” exposures of Section 14.1.

Note: The exposures described in Sections 14.1 and 14.2 are essential for the correct operation of the data pipeline and must be taken as the start of each night.

15.3 Wavelength Calibration

Wavelength calibration is performed using the old DBS arc filters located on the instrument rotator. The Neon/Argon lamp is a good compromise to use at all wavelengths but the Copper/Argon lamp is also useful. Use the standard science aperture for wavelength calibration frames. The line lists are given in: (<http://www.mso.anu.edu.au/~bessell/FTP/Spectrophotometry/>)

The names of the files are:
nearw.arc – A line list for the NeAr lamp (with W contaminants)
cuarti.arc – A line list for the CuAr lamp (with Ti contaminants).

Please note: Although the camera is fully thermally compensated for focus and for scale against changing temperature, the dispersion of the gratings changes with temperature. Because the grating spacing increases with temperature, spectra are shifted towards the blue as temperature increases. The effect is about 0.14 pixels/ degree C for the B3000 grating and 0.36 0.14 pixels/ degree C for the R3000 grating. The effect should be linear with temperature change. Thus, for precision velocity measurements it is important to obtain a matching set of arc observations.

15.4 Flux Calibration

If you want to undertake absolute spectrophotometric calibration, then additional calibration frames need to be taken during the observing. These fall into two categories: (1) Black-Body standards and (2) Absolute calibration standards, although for both of these the technique of observation is exactly the same. We recommend that you take three exposures of your calibration sources and then combine them to remove cosmic ray events.

The list of recommended WiFeS standards is given in Table 19. For UV observations it might be necessary in addition to use the UV -strong standards given by Bessell, M.S. 1999 PASP, 111, 1426-1433 (*see* Table 5).

For the list of all data needed to perform the spectrophotometry go to:

<http://www.mso.anu.edu.au/~bessell/FTP/Spectrophotometry/>.

The file AAREADME contains a description of the files and their content.

Star	RA	Dec(J2000)	V	B-V	Notes
VMa2					
HD 9051	00 49 10.0	+05 23 24	12.38	0.550	WD: DG: Bessell Standard
HD 16031	01 28 46.5	-24 20 25.4	8.93	0.820	
HD 26169	02 34 11.0	-12 23 03.5	9.77	0.437	near Magellanic Clouds, a Bessell Standard
HD 26297	04 00 52.5	-75 36 11.4	8.90		
HD 29574	04 09 03.4	-15 53 27.1	7.46	1.088	
HD 36702	04 38 55.7	-13 20 48.1	8.33	1.304	
HD 44007	05 31 52.2	-38 33 24.0	8.33	1.148	
HD 55496	06 18 48.5	-14 50 43.4	8.05	0.829	
L 745-46a	07 12 11.4	-22 59 00.6	8.37	0.955	
BD -12 2669	07 40 21.0	-17 24 54.0	13.03	0.245	WD: DF: Bessell Standard: Ca HK lines, a very weak NaD 2% deep & Halpha 5% deep.
HD 83212	08 46 39.6	-13 21 25.4	10.24	0.311	
LTT 4364	09 36 20.0	-20 53 14.8	8.33	1.015	
G13-35	11 45 43.0	-64 50 24.0	11.51	0.190	WD: DC(C2): Bessell Standard: <i>Black-body standard</i>
HD 118055	12 25 35.0	+01 17 02.3	9.66	0.445	
HD 122956	13 34 39.9	-16 19 22.7	8.86	1.268	
HD 128279	14 05 13.0	-14 51 25.5	7.22	0.939	
G20-15	14 36 48.5	-29 06 46.7	8.02	0.640	
HD 161770	17 47 28.0	-08 46 47.7	10.60	0.605	
HD 165195	17 47 46.1	-09 36 18.5	9.68	0.672	
EG 131	18 04 40.1	+03 46 44.7	7.31	1.232	
HD 184266	19 20 35.0	-07 40 06.0	12.28	0.040	WD: DC: <i>Blackbody Standard</i> 11800K. Very weak Halpha line about 5% deep.
HD 187111	19 34 15.4	-16 19 00.2	7.59	0.548	
G24-3	19 48 39.6	-12 07 19.7	7.71	1.171	
CD -30 18140	20 05 44.3	+04 02 52.8	10.46	0.510	
HD 204543	20 44 06.3	-30 00 07.6	9.94	0.428	
G29-23	21 29 28.2	-03 30 55.4	8.28	0.888	
LTT 9491	23 19 40.5	+03 22 16.7	10.21	0.456	
F 110	23 19 35.0	-17 05 24.0	14.10	0.030	Hot: HST Standard: Hamuy
	23 19 58.0	-05 09 54.0	11.85	-0.304	V: Hot UV-strong star : HST Standard: Hamuy

Fig. 19.— Recommended flux standards. The standards in **Bold Face** are the primary standards to use.

16 WiFeS data reduction pipeline

16.1 Overview

A data reduction software pipeline has been developed to implement standard data reduction procedures for WiFeS data. This software is in the form of an external IRAF¹ package that is based on, utilises and extends the capabilities of the Gemini Observatory’s `gemini IRAF` package². The `wifes` package consists of a set of tasks that are designed to process the WiFeS integral field spectroscopic data, and are layered over the `gemini` processing tasks and the other IRAF functions that these implement. To use the `wifes` package and data reduction pipeline therefore requires a current IRAF installation: version 2.14 or later (the package has been tested with version 2.14.1), and the current version of the GEMINI package: version 1.9.1 (which has its own prerequisites, as described on the Gemini Observatory web pages).

The spectroscopic data reduction functions in IRAF are accessed (generally through `gemini` intermediate tasks) by `wifes` tasks that handle the optical integral field data format of WiFeS. The pipeline converts the raw WiFeS data to multi-extension FITS format (MEF), which is appropriate for storing the data that result from the multiple apertures (slitlets) of an integral field instrument, and is the data format expected by the `gemini` package. After preliminary data checking and preparation, the raw spectra corresponding to each slitlet in the instrument field of view are extracted and moved to individual image extensions and may each be associated with corresponding data quality and variance image extensions. These individual one-dimensional spectra are processed using long-slit data reduction procedures, before, in the case of science spectra, being assembled into a three-dimensional data cube with two spatial dimensions and one spectral dimension.

The data reduction package includes a set of wrapper tasks that provide a simple way to set up and invoke the standard reduction procedures that will be applicable to most data sets. A pre-processing task, `wftable`, is provided to reformat and assist in organising sets of raw image files produced by WiFeS. `wftable` converts the simple FITS raw images into MEF files, prints summary

tables of files in the raw data directory and compiles text file lists that group images of the same type (e.g. flats, arcs, object images etc.). These lists are used by the other top level tasks to identify the set of images to be included in a given data reduction session.

The `wfcal` task provides options for processing calibration data. The task produces ground and sky flat field images, bias (or zero) frames, arc lamp images for calibrating the wavelength scale and coronagraphic (wire) images for correcting and aligning spatial coordinate systems, and derives the solutions for wavelength and spatial calibration.

A complete set of processed calibration data for each camera and grating combination is also provided with the `wifes` package. These will be regularly updated by RSAA observers and made available to users, so that, when required, recent calibration data sets can be used in place of calibration data obtained during a user’s observation run. These calibration sets are also utilised, by default, during the ‘quicklook’ mode of the `wfreduce` task, discussed briefly below.

Science, or ‘object’, observations are processed using the `wfreduce` task. The procedure prepares object frames for reduction: trimming data, combining frames, subtracting a bias frame, flat-fielding and subtracting the sky signal from the image data. By selecting various combinations of the input options, the task can be used to process observations of standard stars, to extract the information needed for flux calibration and to correct telluric effects in target object spectra. When required, the task applies the solutions for spectral and spatial calibration provided in the output from `wfcal` (or from the default calibration set), performs both a telluric correction and a flux calibration, and corrects for differential atmospheric correction. At the end of processing a given set of data, `wfreduce` produces the data cube, (25 × 76) spatial pixels × 4096 spectral pixels in size, constructed from the reduced data set. The `wfreduce` task can be configured to run in ‘quicklook’ mode, which is designed to provide a view of WiFeS data while the observer is at the telescope using the instrument. In this mode the task performs minimal processing, applies standard calibration solutions and constructs a preliminary data cube from which a projected image is extracted and displayed.

Two other independent tasks are planned to be included in the `wifes` package operate on the output data cubes. `wfcombine` will combine reduced WiFeS data cubes both to increase signal-to-noise or to extend wavelength coverage and `wfmosaic` will provide a means to mosaic a number data cubes that cover adjacent or overlapping fields on the sky.

¹ Image Reduction and Analysis Facility; IRAF is distributed by the National Optical Astronomy Observatories, which are operated by the Association of Universities for Research in Astronomy, Inc., under cooperative agreement with the National Science Foundation.

² <http://www.gemini.edu/sciops/data-and-results/processing-software>

17 Installing the package

1. Download the current IRAF WiFeS package from the ANU/RSAA ftp site: the package is temporarily available from `ftp://mso.anu.edu.au/~cfarage/wifes_package/wifes.tar.gz`. The WiFeS package contains IRAF scripts, data files, standard calibration data and documentation files. Extract the subfolders and files to a location on your local system where users have read and execute permissions.
2. The WiFeS package scripts rely on tasks in the Gemini IRAF package (particularly the `gemini.gnirs` and `gemini.nifs` sub-packages), which must therefore be installed before the WiFeS scripts can be used. Gemini version 1.9.1 or later is required, and is available, with installation instructions, from: `http://www.gemini.edu/sciops/data/dataSoftware.html`.
3. To install the WiFeS package, you need to set some package-level variables. This can be done using either of the following options:

- (a) Adding the following lines to your `iraf$hlib/extern.pkg` file (this will cause `wifes` to be listed as an available package when IRAF is loaded)

```
set wifes = "/<path-to-wifes-scripts>/"
task wifes.pkg = "wifes$wifes.cl"
task $expand $tr = "$foreign"
and in the helpdb section of that file add:
,wifes$helpdb.mip
```
- (b) Including the following lines in your `login.cl` or `loginuser.cl` file (in this case the package will not be printed in the list of available packages at startup):

```
set wifes = "/<path-to-wifes-scripts>/"
task wifes.pkg = "wifes$wifes.cl"
task $expand $tr = "$foreign"
reset helpdb = (envget("helpdb") //
",wifes$helpdb.mip")
```

18 Setting up for data reduction

It is assumed here that you are already familiar with the basic use of IRAF - you should refer to online tutorials (e.g. `http://iraf.net/irafdocs/`) if necessary.

- Open an 'xgterm' window, and increase its width to at least 150 screen pixels. Start IRAF (from your IRAF directory) with the "ecl", "ncl" or "cl" command, as per your IRAF installation.

- Load the `wifes` package at the IRAF command line:

```
cl> wifes
```

This will load other required packages: `images`, `imutil`, `gemini`, `gemtools`, `gnirs`, `nifs`.

- Before running the `wifes` scripts, start an image viewer (eg. DS9). This will be needed during the data reduction process. You can start DS9 as a background process from a terminal shell ("`> ds9 &`"), or from within IRAF as a foreign task ("`cl> !ds9 &`").

- Set up the `wifes` package environment by editing the package parameters:

```
cl> epar wifes
```

This requires that you select locations for your raw and reduced data files, and any user-created calibration, telluric and flux standard files.

You will need to set some or all of the following `wifes` path name parameters:

- `wfsraw` = "`<path-to-raw-data-files>/`"
`wfcal` and `wfreduce` look for the raw image files and files lists in this location
- `wfsred` = "`<path-to-reduced-data-files >/`"
This is the destination for most of the output files produced by `wfreduce`. It is probably best to provide different directories in `wfsred` and `wfsraw`; if you want to keep everything in one place, create a subdirectory for the reduced data.
- `wfscal` = "`<path-to-standard-calibration-files >/`"
Calibration library data are sought here by `wfreduce` if the input parameter `calchoose` is set to "no". The default is the calibration data directory in the `wifes` package: `wifes$cal/`.
- `wfstel` = "`<path-to-standard-telluric-calibration-files >/`"
Telluric calibration library data are sought here by `wfreduce` if `calchoose` = no. The default value is `wifes$stel/`
- `wfsflux` = "`<path-to-standard-flux-calibration-files >/`"
Flux calibration library data are sought here by `wfreduce` if `calchoose` = no. The default is `wifes$stel/`

- `wfscaluser = "/<path-to-user-created-calibration-files >/"`
This is the output directory for `wfcal` if that task's own output directory parameter (`wfcal.outdir`) is not defined. `wfreduce` seeks calibration data here if `calchoose=yes`.
- `wfsteluser = "/<path-to-user-created-telluric-and-flux-data >/"`
`wfreduce` will use this directory for output files from steps that derive the flux calibration and telluric correction data. In addition, the the parameter `calchoose` is set to `yes`, `wfreduce` looks here for the input data to be used during the steps that apply the flux and telluric calibrations to a science object data set.

Basic calibration files can be created using the `wfcal` task. If you decide instead to use files from the standard calibration library provided, you will only need to run the task `wfreduce`, setting the `calchoose` parameter to "no".

- WiFeS reduction tasks produce logging information describing the progress and outcomes of the processing tasks performed. By default, the principle logfile to which this information is written, is called "wifes.log", but this may be changed at the package level by editing the logfile parameter in the `wifes` task (by running "cl> epar wifes"), or by changing the default name in the package file `wifes.dat`, located in the `wifes` package data directory: "wifes\$data/wifes.dat".

You are now ready to reduce your WiFeS data. The following section provides some background information about the instrument and the format of the raw data files.

19 WiFeS data format

The WiFeS IRAF package contains the tasks needed for processing WiFeS integral-field spectroscopic data. Descriptions of the individual tasks can be found in their help files (the command "help wifes" lists those tasks with associated help files), and those of the subsidiary tasks that are used. The task `wifexamples` provides a set of sample data reduction recipes.

The raw data files obtained during a WiFeS observing run (all target object, standard star and calibration images) are each assigned a unique observation ID that is written to the FITS file header `OBSID` keyword and will form the standard file name when the

data are downloaded through the TAROS Observation Database. This ID string has a standard format generated from a UT date/time stamp and identifying the camera that produced the file:

T2m3< *xx* >.YYYYMMDD.HHMMSS.fits

where *xx* are characters that represent the camera of origin: 'wr' for the WiFeS red camera, 'wb' for the WiFeS blue camera and 'Ap' for the field viewing camera; and YYYYMMDD represents the date and HHMMSS the time associated with the file's creation.

The layout of a raw WiFeS image is shown in Fig 3. There are four detector quadrants (A, B, C, D) and each is read out through a separate amplifier with overscan columns at the left and right. The horizontal axis is the dispersion axis, and the vertical axis contains the 2D sky plane in 25 horizontal slices (*x*-axis on sky) each of 76 pixels (*y*-axis on sky). Effectively, the image slicer turns 25 adjacent slits into a stack of wavelength-dispersed slices each 38 arcsec long (76 pixels). Each complete slice has 76 pixels of object, a 4 pixels gap, 76 pixel of shuffled (or sky) data and a further 4 pixel gap to the next slice.

The data reduction pipeline reconstructs the raw, dispersed data into a data cube consisting of a stack of wavelength calibrated image planes. The instrument provides a nod and shuffle mode in which the 'on-object' slices on the detector are interleaved with 'sky' observations in the secondary slit positions (see Section (13), above).

WiFeS raw images are single-extension FITS files, but are converted by the WiFeS data reduction pipeline script `wftable` to multi-extension FITS (MEF) files with two file extensions. Header information is written to the primary header unit (PHU) in extension [0], and image data is placed in extension [1]. The WiFeS pipeline tasks add header information during processing to document important parameter values and the data reduction steps that have been completed.

Pre-processing with package task `wfprepare` trims the overscan regions from the images, after optionally using it to subtract an averaged bias signal, and generates and adds variance [VAR] and data quality [DQ] extensions to the files. The data quality plane allows bad pixels to be flagged for subsequent data reduction steps. `wfprepare` writes some information to the image headers for use in later processing steps and attaches the relevant Mask Definition File (MDF) from the package data directory as a FITS table extension. The MDF defines the pattern of image slices on the detector and how these regions map to the sky field.

During the reduction, the images are 'cut' - the regions corresponding to each of the focal plane slices are extracted and placed in individual file extensions.

Science (SCI), variance (VAR) and data quality (DQ) planes are produced for each of the 25 IFU slices, so data files in intermediate data reduction stages have 77 extensions - the PHU, MDF and 25 SCI, VAR and DQ extensions. The Gemini task `gemextn` can be used to display the extensions present in a given MEF file. An example `gemextn` output for a cut WiFeS image could look something like:

```
cl> gemextn T2m3wr.20090101.012345_R3000_res
T2m3wr.20090101.012345_R3000_res[0][PHU]
T2m3wr.20090101.012345_R3000_res[1][MDF]
T2m3wr.20090101.012345_R3000_res[2][SCI,1]
T2m3wr.20090101.012345_R3000_res[3][VAR,1]
T2m3wr.20090101.012345_R3000_res[4][DQ,1]
T2m3wr.20090101.012345_R3000_res[5][SCI,2]
...
T2m3wr.20090101.012345_R3000_res[76][DQ,25]
```

This lists both the index (within the first set of square brackets) and the name and slice (within the second) for each extension. It is only necessary to use one of these when referring to a file extension, since either uniquely identifies it. The final product of the `wfreduce` pipeline script is an MEF file with a single image extension that contains a reconstructed data cube (x, y, λ), with calibrated world coordinate systems in the data extension header. This data can be read into a data visualisation program (e.g. Matlab, Scilab or Euro3D) for further analysis.

20 WiFeS Data Reduction

The WiFeS package contains the tasks needed for processing WiFeS integral-field spectroscopic data. The specifics of the individual tasks can be found in their help files (`'help wifes'` lists those tasks with associated help files). This document describes the common features of the top-level tasks and gives a description of the WiFeS data format³. The command `'wifexamples'` provides sample data reduction recipes.

Typically a user will obtain a set of raw images during an observing run comprising object observations and various calibration images (arcs, flats, etc.). The standard file naming system for these files is in 3 parts - the telescope name (T2m3), and camera name (red is 'wr', blue is 'wb'), and the UT date and time:

T2m3wr.YYYYMMDD.HHMMSS.fits

The layout of a raw WiFeS image is shown in Fig 3. There are four CCD quadrants (ABCD), each read through separate amplifier, with overscan columns at the left and right. The horizontal axis is the dispersion (wavelength) axis, and the vertical axis contains the 2D sky plane in 25 horizontal slices (x -axis on sky) each of 76 pixels (y -axis on sky). Effectively, the image slicer turns 25 adjacent longslits into a stack of wavelength-dispersed slices each 38 arcsec long (76 pixels). Each complete slice has 76 pixels of object, a 4 pixels gap, 76 pixel of shuffled (or sky) data and a further 4 pixel gap to the next slice.

The purpose of the image data reduction pipeline is to reconstruct the focal plane data into a data cube consisting of a stack of wavelength calibrated image planes. The instrument provides for a nod and shuffle mode so the on-object slices are interleaved with 'sky' slices (see Section (13), above).

WiFeS raw images are single-extension FITS files, but are converted by the WiFeS data reduction pipeline script `'wfable'` to multi-extension FITS (MEF) files containing two extensions. Header information is written to the primary header unit (PHU), which is extension [0], and image data is placed in extension [1]. The WiFeS pipeline tasks add header information during processing to document the data reduction steps that have been completed and important parameter values.

Pre-processing with `'wfprepare'` renames the data extension [SCI] and adds variance [VAR] and data quality [DQ] extensions. The data quality plane allows bad pixels to be flagged for subsequent data reduction steps. Various header keywords are added by `'wfprepare'` for use in later processing, together with an MDF FITS table extension defining the WiFeS pattern of image slices on the detector and how the slices map to the sky field.

The WiFeS data reduction pipeline cuts the image slices into SCI, VAR and DQ planes for each of the 25 different slices in the IFU. So, WiFeS data at the intermediate data reduction stage has 77 extensions - [PHU,0], [MDF,1], 25 SCI, 25 VAR and 25 DQ. The task `'gemextn'`, when used with default parameters and no arguments, will display all the extensions present in a file:

```
> unlearn gemextn
> gemextn T2m3.20080109.013344
T2m3.20080109.013344[0][PHU]
T2m3.20080109.013344[1][MDF]
T2m3.20080109.013344[2][SCI,1]
```

³Abbreviations used

WiFeS – Wide Field Spectrograph

NIFS – Near-IR Integral Field Spectrograph

IFU – Integral field unit

MDF – Mask definition file (a binary FITS table)

MEF – Multi-extension FITS file

PHU – Primary header unit (extension [0] of a MEF file)

```
T2m3.20080109.013344[3][VAR,1]
T2m3.20080109.013344[4][DQ,1]
T2m3.20080109.013344[5][SCI,2]
...
T2m3.20080109.013344[76][DQ,25]
```

This includes both the index (inside the first `[]`) and the extension name and slice (second `[]`). It is only necessary to use one of these, since either uniquely identifies an extension.

The final product of the `wfreduce` pipeline script is a data cube (x, y, λ) in an MEF file. This data cube can be read into a data visualisation program (*e.g.* Matlab, Scilab or Euro3D) for further analysis and plotting.

21 WiFeS Pipeline Scripts

The top-level WiFeS package scripts provide an interface to the processes and tasks required to reduce the WiFeS data. These primary tasks are:

wftable – Provides an on-screen text summary of the raw data files in a directory, and creates list files, which define the files to be processed and are accessed by the **wfcal** and **wfreduce** tasks.

wfcal – Produces a set of calibration files for use with **wfreduce**. This is not necessary if you are using the standard calibration file sets that are provided with the WiFeS pipeline, but may be preferred for improved data reduction quality. Calibration data (flat field, arc lamp, bias images etc.) obtained during your observing run are processed, and calibration solutions obtained, with this task.

wfreduce – Processes object images for a specific set of observations and applies calibrations derived with **wfcal**. This script is also used to derive and apply flux calibration information and correct for telluric features in object spectra using standard star observations, perform sky subtraction, and produce and inspect the final data cube from the reduced data.

Several tasks, for combining multiple 3D data sets, are planned as future additions to the WiFeS package:

wfcombine – For combining reduced data cubes; e.g. to increase signal-to-noise or extend wavelength coverage.

wfmosaic – For producing a spatial mosaic of a number of WiFeS reduced data cubes, with adjacent or overlapping fields on the sky.

21.1 WFTABLE: Setting up for data reduction

USAGE

```
cl> wftable
cl> wftable grating=<grating_name>
cl> wftable grating=<grating_name>
dichroic=<dichroic_name>
```

PARAMETERS

grating = <grating_name> : WiFeS grating (U7000, B7000, R7000, I7000, B3000 or R3000) A grating identifier is given here to define the set of files to be described and included in list files (name may be given as upper or lower case)

dichroic = <dichroic_name> : WiFeS dichroic (RT480, RT560, RT615)

A dichroic (beam splitter) identifier (may be upper or lower case) can also be provided to constrain the set of

files to be described and included in the lists. If this parameter is not specified when a **grating** value is, the ‘standard’ combination for the grating will be assumed.

DESCRIPTION AND INSTRUCTIONS

wftable tabulates key data from raw image file headers, reformats raw data into MEF files and creates reduction file lists to which **wfcal** and **wfreduce** refer.

When implemented, this script examines all FITS files in the current directory. If no parameters are given, the first output is a tabular summary of the unique combinations of camera, grating and dichroic settings that exist among the image files in the directory. For example, if a directory contained files from a set observations made using the B7000/I7000/RT615 grating and dichroic combination with both cameras, and another using the R3000/B3000/RT560 configuration but only the blue camera, the tabulated summary produced would contain the following information:

CAMERA	GRATINGB	GRATINGR	BEAMSPLT
WiFeSBlue	B7000	I7000	RT615
WiFeSRed	B7000	I7000	RT615
WiFeSBlue	B3000	R3000	RT560

This provides an overview of the different instrument configurations used to obtain the set of data in the current directory. Although there are no red camera images present to which the R3000 grating setting is relevant, this grating is still listed since the headers of the blue camera images also record the red grating setting in the **GRATINGR** keyword.

A more detailed summary of image data is then printed for each FITS file in the directory. Information including the filename, observation ID, observing mode, image type, object name, grating, dichroic, right ascension, declination, instrument position angle, exposure time and airmass are obtained from the header and listed on the screen (by default the standard output). When raw single extension image files are encountered, the **wfreformat** task is invoked to reformat the data as an MEF file consisting of a PHU and single data extension ([SCI,1]). This process can take some time to complete if there are many files in the directory, but the reformatting is skipped for files found to be in the MEF format already. The files will also be renamed to filename formats matching the observation ID (**OBSID** keyword values), with the difference that the full stop characters are replaced by underscores.

21.2 WFCAL : Calibrating the Data

USAGE

wfcal (Performs Calibrations)

PARAMETERS

dounlearn = no : Unlearn all Gemini parameter sets?

ddowfprepare = yes : Redo wfprepare steps?

dogflat = yes : Create ground flat field frame?

dozero = yes : Redo wfprepare steps?

doarc = yes : Create wavelength calibration?

dowire = yes : Create distortion calibration?

dosflat = no : Create sky flat field frame?

outname = "" : Output file root (no spaces, filename format with no extension)?

outdir = "" : Output directory for calibration files?

If the input value is an empty string (default), the directory 'caluser', inside your 'wifes.wfsred' directory will be used (it will be created if it does not already exist).

reference = "" : File name for slitlet geometry?

If you leave this empty, wfcal will choose the appropriate refflat_GRATING file name to use as output
keepfiles = no Keep intermediate data reduction files?

This could rapidly fill up your available disk space, so only set this parameter to yes if you are encountering problems.

answer = yes : OK to continue?

DESCRIPTION AND PROCEDURES

The WiFeS pipeline calibration data reduction is accomplished by running the the wfcal task on a list of calibration files generated by the wftable task (see relevant help file). The user can create their own calibration data using the task wfcal, or simply use the calibration products provided by the WiFeS support team. The key wfcal steps are as follows:

- Prepare IRAF, set hidden parameters/variables
- Prepare/reduce ground flats
- Prepare/reduce sky flats
- Prepare/reduce and combine zero frames
- Prepare/reduce arc and determine wavelength solution
- Trace spatial curvature in wire image
- Clean up

You should also refer to the calibration cookbook, which can be accessed by issuing the command: wifesexamples.

Before you can run wfcal, you must start DS9 because the pipeline script needs to display images and obtain user-provided cursor input during the calibration process. wfcal provides on-screen progress information and this is also recorded in the various logfiles. Several reduction steps are interactive, requiring input in the IRAF terminal, on the graph display screen or on the DS9 image screen.

A number of parameters (described above) need to be set before running wfcal. Initially, this is best done with:

```
> unlearn wfcal
> epar wfcal
```

Subsequently, the few parameters that may change between wfcal runs can be set at the command line (*e.g.*):

```
> wfcal dowfprepare+ dogflat- .....
```

To return to the default parameter values (always safest), use the command:

```
> unlearn wfcal
```

Various intermediate and temporary files are created as part of the calibration process. These are deleted as part of the automatic cleanup routine (invoked if the script halts execution or safely completes), unless you set the wfcal keepfiles parameter to "yes" (or keepfiles+).

The wfcal calibration steps are quite separate from the data reduction process. They perform the following functions:

- **Prepare IRAF, set hidden parameters and variables:** Sets up logfiles, obtains WiFeS-specific keyword information and sets hidden parameters/variables. Switches to the calibration directory where output files will be written (i.e. caluser directory).
- **Prepare ground flats and determine shifts:** This wfprepares the spectral geometry reference image and the ground flat (lamp on) images. It then combines and cuts the ground flats using wfnreduce. We then form the ground flat using wfflat. Finally, we normalise slitlets using the pseudo-"sky" flat and wfsplitfunction.
- **Reduce the sky flats:** This wfprepares each skyflat and image and then combines and cuts using wfnreduce. We then form the sky flat with wfflat and normalize slitlets with wfsplitfunction.

- **Reduce and combine the zero or bias frames:** This wfprepares each zero (bias) image, and makes a median averaged combined bias.
- **Reduce arc and determine wavelength solution:** This wfprepares each arc image, and combines them using a median average. This image is then cut with wfnsreduce and wavelength calibrated with wfwavelength.
- **Trace the spatial curvature of each slit:** This uses the “wire” image obtained using the Coronagraphic aperture mask. First, we wfprepare the wire image and each ground flat image, We combine the ground flat (lamp on) image and we construct an assymmetric 3-wire image to provide scale. Then we subtract the “wire” frame from the combined ground flat frame to create a positive “virtual star” trace. This is reduced with wfnsreduce and we establish the S-distortion calibration with nfsdist. The output is written to the database folder.
- **Clean up:** All temporary files are deleted.

21.3 WFREDUCE: Reducing the Data

USAGE

wfreduce

PARAMETERS

The following parameters determine which steps in the data reduction are carried out:

dounlearn = no

Unlearn all gemini,gemtools,gnirs,nifs parameter sets?

This will only be necessary if they have been changed since the wifes package was loaded in the current session.

dowfprepare = yes

Redo wfprepare steps?

wfprepare pre-processes each raw data file listed in the "list_obj" text file created by wftable. The output images are prefixed with the letter "n". Set this parameter to "no" if you know you have already wfprepare'd these files - however wfprepare will in any case check for the presence of the WFPREPARE header keyword to avoid duplicate processing.

docombine = yes

Median combine multiple wfprepare'd object images?

It is safe to leave this set to yes, even if you only have one object image.

dozero = yes

Subtract median-averaged zero created with wfcalscl to remove pixel-to-pixel bias from the combined object image?

dosubshuffled = yes

Subtract shuffled sky if in Nod and Shuffle mode?

The pipeline checks that the observing mode is recorded in the combined image header as

NOD_AND_SHUFFLE. If the mode is not Nod and Shuffle, this parameter should be set to no, and the dosubsky parameter set to yes (see later). A scaling factor (input parameter skyfactor) can be applied to the sky image prior to subtraction, but in normal circumstances this will be set to 1.000.

doreduce = yes

Reduce the combined object image?

This involves cutting the image into 25 horizontal slices, and flat-fielding. Each of the 25 image slices will have its own VAR and DQ extensions.

dofixbad = yes

Fix bad pixels flagged in DQ array? This task uses fixpix to interpolate over the bad pixels in the narrowest direction. It may take some time to complete.

dofitcoords = yes

Fit 3D user coordinates to correct for spectral and spatial distortion? This task uses a wire image from the calibration directory.

dotransform = yes

Produce transformed 3D data cube using nftransform?

dosubsky = yes

Define rectangular sky region within cube and subtract averaged sky spectrum? This is only relevant for Classical observing mode.

dotelextract = no

Extract a telluric star spectrum? If set to yes, the output file is written to the calibration telluric directory.

dofixa0 = no

Fix A0 telluric star absorption?

dotelcorrect = no

Apply telluric correction to data cube?

dofluxextract = no

Extract a flux standard spectrum?

This creates a flux standard image that can be used to apply flux calibration to the data cube - see the `dofluxcalibrate` parameter.

`dofluxcalibrate = yes`

Apply previously created flux standard calibration to data cube?

`dodar = yes`

Apply correction to data cube for differential atmospheric refraction (DAR)?

`doscience = yes`

Extract a science object spectrum? A 2D image is displayed of a spectral slice through the data cube. The limits of the spectral slice are determined by the `waverest`, `redshift`, `vstart` and `vstop` parameters (see later). The user is asked to mark in DS9 the centre (peak emission) of a region having aperture radius determined by parameter `sciaper`. A summed, full-range spectrum is then extracted from the cube within this aperture. The 1D output spectrum is saved in an image file with “_sci” suffix.

`donf3d = yes`

Output a simple FITS cube for NF3D? The flux-calibrated signal is scaled up by an arbitrary factor, and the cube is output to an image file with suffix “_res_c”.

`dothroughput = yes`

Plot throughput over band? The plot is saved to an image file with suffix “_res_thr”.

The following parameters provide input information to the reduction pipeline:

`calchoose = no` –Use your own calibration data (in `caluser` directory as set by “`epar wives`”)? If “yes”, the user must enter relevant values for parameters `reftrans`, `refflat`, `flat`, `zero`, `arcwave`, `wire`. If “no”, the correct standard calibration data is automatically selected based on the `GRATING` and `CAMERA` keywords in the object files.

`telchoose = no` –Use your own telluric data (in `teluser`)?

`keepfiles = no` –Keep intermediate data reduction files? This could rapidly fill up your available disk space, so only set this parameter to yes if you are encountering problems.

`skyfactor = 1.000` –Factor by which to scale noded sky frame? This should be set to 1.000 unless the shuffled sky slices have an exposure time that differs from the unshuffled object slices.

`reftrans = ""` –File defining coordinate transformation?

The following parameters are used to extract a 1D spectrum from the reduced data cube:

`sciaper = 5.0` –Science object aperture diameter (arc-sec)? This is the diameter of the circular area that is integrated to produce a representative 1D spectrum from the data cube. You will be asked to mark the centre of this aperture (peak of the flux) in DS9 as part of the `doscience` subtask.

`emission = yes` –Spectral feature is an emission line?

`waverest = 0.65628` –Feature rest wavelength (microns) normally set to `red(Halpha) = 0.65628` or `blue(Hbeta) = 0.48613`?

`redshift = 0.05` –Object redshift? This is used with `vstart` and `vstop` parameters to fix a region within the data cube for extraction of the 1D science spectrum.

`vstart = -200.0` –Start velocity range (km/s)?

`vstop = 200.0` –Stop velocity range (km/s)?

The following parameters, some of which may be ignored if `calchoose=no`, locate the source and settings of required calibration data:

`refflat = ""` –Flat field file defining slitlet geometry? If this parameter is left empty (default), the standard calibration file `refflat_GRATING.fits` is used.

`flat = ""` –Flat field file name? If this parameter is left empty (default), the standard calibration flat file for this grating is used.

`zero = ""` –Averaged zero file name? If this parameter is left empty (default), the standard calibration zero file for this camera is used.

`arcwave = ""` –Wavelength calibrated arc file name? If this parameter is left empty (default), the standard calibration `arcwave` file for this grating is used.

`wire = ""` –Wire file name? If this parameter is left empty (default), the standard calibration `wire` file for this grating is used.

`skyfile = "WIFESoh.dat"` –Sky line list file name?

`telluric = ""` –Telluric calibrator filename?

`telaper = 5.0` –Telluric aperture diameter (arcsec)? Size of aperture for integration of flux, centred on the point marked by the user in DS9 when extracting a telluric standard (`dotelextract`).

`tellfile = "Vegalines.tab"` –Telluric star absorption line list table? This is in a special format, but you can view its contents with a `tprint` command (see `help tprint`).

`fluxstd = ""` –Flux standard filename? If you have set the parameter `dofluxcalibrate=yes`, then the setting of this parameter depends on your setting of the `telchoose` parameter. if `telchoose=yes` you must enter a flux calibration file name relevant to the object `GRATING`, and contained in the user calibration directory. If `telchoose=no` leave this parameter blank as the pipeline

will find the correct flux calibration file in the standard calibration directory.

fluxaper = 10.0 -Flux standard aperture diameter (arc-sec)? Size of aperture for integration of flux, centred on the point marked by the user in DS9 when extracting a flux standard (dofluxextract).

fluxmag = 8.00 -Flux standard magnitude?

fluxband = "B" -Flux standard mag band (U|B|R|I)?

fluxteff = 10000.0 -Flux standard temperature (K)?

answer = no -Accept this result?

21.4 Description of Reduction Procedures

Examples of the reduction process for the various modes can be printed with the command: wifsexamples.

Before running the `wfreduce` task please note the following:

1. Before you run `wfreduce` you must start DS9 because the pipeline script needs to display images and obtain user-provided cursor input during the reduction process.
2. `wfreduce` provides on-screen progress information and this is also recorded in the various logfiles. Several reduction steps are interactive, requiring input in the `iraf` terminal, on the graphics display screen or on the DS9 image screen.
3. A number of parameters (described above) need to be set before running `wfreduce`. Initially, this is best done with:

```
> unlearn wfreduce
> epar wfreduce
```

Subsequently, those parameters that may change between `wfreduce` runs can be set at the command line (*e.g.*):

```
> wfreduce dowfprepare+ dozero- .....
```

To return to the default parameter values (always safest to do so), use the command:

```
> unlearn wfreduce
```

4. Various intermediate and temporary files are created as part of the data reduction. These are deleted as part of the automatic cleanup routine (invoked if the script halts execution or safely completes), unless you set the `wfreduce` `keepfiles` parameter to "yes" (or `keepfiles+`).
5. Before you run `wfreduce`, you must have run `wftable` in the relevant raw data directory in order to write the file lists that `wfreduce` will work on.
6. The `wfreduce` data reduction steps are quite separate from creation of calibration data. They are given below.

The WiFeS pipeline data reduction is accomplished by running the `wfreduce` task on a list of object files generated by the `wftable` task. The data reduction steps

are separate from the creation of calibration data using the task `wfcal` (or simply using the standard calibration products provided with the WiFeS Pipeline package).

The key `wfreduce` steps are as follows:

Stage A: Dealing with individual raw images

- **Set up:** Generate logfiles and obtain WiFeS-specific keyword information. Set hidden parameters/variables and determine the sequence of input files to be processed. Copy arc and wire calibration files from the calibration to the reduction directory.
- **Prepare images for reduction:** Validate image, add various keywords and values (shift, gain, etc.), attach a bad pixel mask, create the variance and data quality extensions, remove the time-dependent bias, trim overscan and detect/remove cosmic rays. Processed images are prefixed with the letter `n`.
- **Combine object images:** validate image, add various keywords and values (shift, gain, etc.), attach a bad pixel mask, create the variance and data quality extensions, remove the time-dependent bias, trim overscan and detect/remove cosmic rays. Processed images are prefixed with the letter `n`.

Stage B: Dealing with combined images

- **Subtract averaged zero:** The pixel-to-pixel averaged zero image (created with `wfcal`) is subtracted from each combined image.
- **Subtract Shuffled Sky:** This applies to `nod` and `shuffle` mode only. In this the shuffled sky slices are shifted and subtracted from object data slices
- **Reduce combined object frame:** This cuts and flat-fields object image. The input file is in the form `"OBSID_GRATING_obj_a.fits"`. The output file is in the form `"OBSID_GRATING_res.fits"`. This file is updated by fixing the bad pixels in the next step.
- **Fix known bad pixels:** This fixes the known bad pixels in the object image.

- **Wavelength calibrate:** Performs the wavelength calibration for each slice of the combined frames
- **Fit user coordinates:** This is based on CCD image of the coronagraph wire aperture. It adds the distortion and dispersion mapping information and a 3D world coordinate system to the output headers of each science extension in the reduced object image. The output file is in the form: "OBSID_GRATING_res.fits".
- **Correct for differential atmospheric refraction:** The weighted mean zenith distance and parallactic angle are computed for the observation. These are then used, together with telescope and atmospheric data, to compute and apply wavelength dependent image shifts in the x, y plane.
- **Extract science object spectrum:** The user will be presented in DS9 with a 2D summed view through the data cube. After marking the centre of a spectrum extraction circle (aperture radius set by parameter `sciaper`), a 1D spectrum is extracted and saved in the form "OBSID_GRATING_sci.fits".

Stage C: Forming & Dealing with the data cube

- **Transform to 3D data cube:** Creates the x, y, λ data cube from separate extensions in reduced data file. The output data cube is given a filename in the form: "OBSID_GRATING_res_t.fits"
- **Specify sky subtraction:** This does not apply to nod and shuffled data. In the "Classical" case there will be no useable sky data in the shuffled slices. This stage allows the user to select a rectangular sky region from within the data cube's $x - y$ plane to be subtracted as sky throughout the data cube.
- **Telluric extraction:** If the target is suitable, a 1D telluric star spectrum is extracted and saved to the "tel" or "teluser" directory, depending on the setting of parameter "telchoose". The output filename is in the form: `newline "OBSID_GRATING_tel.fits"`.
- **Fix A0 star absorption:** This step updates the telluric spectrum created in the previous step by correcting for the stellar absorption profiles.
- **Apply Telluric Correction:** The telluric features are removed to update the data cube "OBSID_GRATING_res_t.fits". See the help file for `nftelluric`.
- **Extract Flux standard spectrum:** This creates a flux standard spectrum from the data reduction of a standard star. The output file has the suffix "_flux.fits".
- **Apply Flux Calibration:** A previously created standard flux calibration data is applied to the data cube.
- **Output simple fits cube:** The scilab task `nf3d` may be used to view and investigate the data cube (not as part of the WiFeS Pipeline). This step will create such a cube and scale up the signal count, resulting in a file of the form "OBSID_GRATING_res_c.fits".
- **Plot throughput over band:** The signal throughput is plotted against frequency across the relevant band, and this 1D plot is saved in the form "OBSID_GRATING_res_thr.fits".
- **Clean up:** Removes unwanted working files.

Additional tasks, `wfcombine` (to combine WiFeS data cubes with separate calibration files possibly obtained on different nights) and `wfmosaic` (to mosaic data cubes together) have been planned, but these are not yet provided in the pipeline. They are planned for inclusion at an early stage.